Geoscience Canada
Journal of the Geological Association of Canada
Journal de l'Association Géologique du Canada

Logan Medallist 8. Trace Elements in Iron Formation as a Window into Biogeochemical Evolution Accompanying the Oxygenation of Earth's Atmosphere

Kurt O. Konhauser, Andreas Kappler, Stefan V. Lalonde and Leslie J. Robbins

Volume 50, Number 4, 2023

URI: https://id.erudit.org/iderudit/1108859ar
DOI: https://doi.org/10.12789/geocanj.2023.50.201

See table of contents

Publisher(s)

The Geological Association of Canada

ISSN

0315-0941 (print)
1911-4850 (digital)

Explore this journal

Cite this article

Konhauser, K., Kappler, A., Lalonde, S. & Robbins, L. (2023). Logan Medallist 8. Trace Elements in Iron Formation as a Window into Biogeochemical Evolution Accompanying the Oxygenation of Earth's Atmosphere. *Geoscience Canada*, *50*(4), 239–258. https://doi.org/10.12789/geocanj.2023.50.201

Article abstract

Iron formations exemplify a type of sedimentary rock found in numerous Archean and Proterozoic supracrustal successions. They serve as a valuable chemical record of Precambrian seawater chemistry and post-depositional iron cycling. These formations accumulated on the seafloor for over two billion years during the early history of our planet, offering a unique opportunity to study environmental changes that occurred during Earth's evolution. Among these changes, one of the most significant events was the shift from an anoxic planet to one where oxygen (O2) became consistently present in both the marine water column and atmosphere. This progression towards global oxygenation was closely linked to the emergence of aerobic microbial metabolisms, which profoundly impacted continental weathering processes, nutrient supply to the oceans, and ultimately, the diversification of the biosphere and complex life forms. In this review, we synthesize two decades of research into the temporal fluctuations of trace element concentrations in iron formations. Our aim is to shed light on the complex mechanisms that contributed to the oxygenation of Earth's surface environments.

GAC MEDALLIST SERIES

Logan Medallist 8.
Trace Elements in Iron Formation as a Window into Biogeochemical Evolution Accompanying the Oxygenation of Earth's Atmosphere

Kurt O. Konhauser[1], Andreas Kappler[2], Stefan V. Lalonde[3] and Leslie J. Robbins[4]

[1]*Department of Earth and Atmospheric Sciences, University of Alberta Edmonton, Alberta, T6G 2E3, Canada*
Email: kurtk@ualberta.ca

[2]*Geomicrobiology, Department of Geosciences, University of Tübingen Tübingen, 72076, Germany*

[3]*European Institute for Marine Studies, CNRS-UMR6538 Laboratoire Domaines Océaniques, Technopôle Brest-Iroise Plouzané, 29280, France*

[4]*Department of Geology, University of Regina Regina, Saskatchewan, S4S 0A2, Canada*

SUMMARY
Iron formations exemplify a type of sedimentary rock found in numerous Archean and Proterozoic supracrustal successions. They serve as a valuable chemical record of Precambrian seawater chemistry and post-depositional iron cycling. These formations accumulated on the seafloor for over two billion years during the early history of our planet, offering a unique opportunity to study environmental changes that occurred during Earth's evolution. Among these changes, one of the most significant events was the shift from an anoxic planet to one where oxygen (O_2) became consistently present in both the marine water column and atmosphere. This progression towards global oxygenation was closely linked to the emergence of aerobic microbial metabolisms, which profoundly impacted continental weathering processes, nutrient supply to the oceans, and ultimately, the diversification of the biosphere and complex life forms. In this review, we synthesize two decades of research into the temporal fluctuations of trace element concentrations in iron formations. Our aim is to shed light on the complex mechanisms that contributed to the oxygenation of Earth's surface environments.

RÉSUMÉ
Les formations de fer sont un exemple de roche sédimentaire que l'on trouve dans de nombreuses séquences supracrustales de l'Archéen et du Protérozoïque. Elles représentent un enregistrement chimique précieux de la composition de l'eau de mer du Précambrien et du cycle du fer post-dépôt. Ces formations se sont accumulées sur le fond marin pendant plus de deux milliards d'années au début de l'histoire de notre planète, offrant une occasion unique d'étudier les changements environnementaux survenus au cours de l'évolution de la Terre. Parmi ces changements, l'un des événements les plus significatifs a été la transition d'une planète anoxique à une planète où l'oxygène (O_2) est devenu constamment présent à la fois dans la colonne d'eau marine et dans l'atmosphère. Cette progression vers l'oxygénation globale était étroitement liée à l'émergence de métabolismes microbiens aérobiques, qui ont profondément influencé les processus d'altération continentale, l'apport de nutriments aux océans et, finalement, la diversification de la biosphère et des formes de vie complexes. Dans cette revue, nous synthétisons deux décennies de recherche sur les fluctuations temporelles des concentrations en éléments traces dans les formations de fer. Notre objectif est de faire la lumière sur les mécanismes complexes qui ont contribué à l'oxygénation des environnements de la surface de la Terre.
Traduit par la Traductrice

INTRODUCTION
The study of ancient sediments, such as iron formations (IF), has generated important insights into the complex interplay

between life and Earth's surface environments throughout geologic history (e.g. Konhauser et al. 2017). Uniquely, most IF are chemical sediments, characterized by high iron (15–40 wt.% Fe) and silica (40–60 wt.% SiO_2) content that were deposited from seawater during the Precambrian. Notably, the Nuvvuagittuq Supracrustal Belt in northern Quebec and the Isua Supracrustal Belt in West Greenland, which date back over 3.75 billion years, contain perhaps the earliest IF and associated sedimentary rocks (Mloszewska et al. 2012; Czaja et al. 2013). The period between 2.7 and 1.9 Ga witnessed the highest abundance of IF. Indeed, Isley and Abbott (1999) estimated that during those 800 million years, perhaps as much as 60% of the global volume of preserved IF was deposited. This timeframe coincides with a significant transition in Earth's oceans and atmosphere towards a partially oxygenated state (Lyons et al. 2014). Iron formations then essentially disappear from the rock record for nearly 1.2 billion years. This gap has been explained by a shift to fully oxic or sulphidic deep-ocean conditions. The earlier suggestion of oxic deep-ocean conditions after ca. 1.88 Ga (Holland 1984) was challenged by the proposal that deep-ocean conditions were predominantly euxinic (anoxic and sulphidic) until full ocean ventilation during the late Neoproterozoic or earliest Phanerozoic (e.g. Canfield 1998). Iron formations reappear again briefly in the Neoproterozoic when oceans returned to a ferruginous state during the ice-covered Sturtian glaciation (Hoffman et al. 1998), with rare instances documented in the early Phanerozoic (e.g. Li et al. 2018).

Classically, IF have been categorized into three main types: Algoma-type, Superior-type and Rapitan-type, based primarily on their depositional environment (Gross 1980). Algoma-type IF are typically found interlayered with, or genetically linked to, volcanic rocks. These volcanic rocks range from ultramafic–mafic to felsic compositions and are commonly accompanied by volcaniclastic greywacke and shale in greenstone belts. In many cases, Algoma-type IF are spatially associated with volcanogenic massive sulphide (VMS) deposits (Bekker et al. 2010). The prevailing belief is that Algoma-type IF precipitated near volcanic arcs and spreading centres through exhalative hydrothermal processes associated with submarine volcanism (Gross 1980). In contrast, Superior-type IF developed in sediment-dominated settings, specifically on the passive margins of continental shelves. Unlike the Algoma-type IF, they lack direct stratigraphic connections with volcanic rocks. Superior-type IF are believed to have been deposited on the outer shelf, but they are often interbedded with, or transition into, carbonate rocks and black shale suggesting their deposition moved landwards with changing sea level (Trendall 2002). Superior-type IF can be laterally extensive (Fig. 1A), with estimates suggesting original aerial extents may have exceeded 100,000 km^2 (Bekker et al. 2010). In terms of mass, the largest Superior-type IF contain over 10^{14} tonnes (10^{17} kg) of iron (Isley 1995), and today serve as a significant source of iron for global iron and steel production (Hagemann et al. 2016). Rapitan-type IF are associated with Neoproterozoic Snowball Earth conditions and are thought to be deposited as a by-product of global-scale glacial activity (Hoffman et al. 1998). Named after the ca. 715 Ma Rapitan Iron Formation in northern Canada, a major feature of these IF is their interbedding with glacial diamictite (e.g. Smith 2018). In a model developed by Klein and Beukes

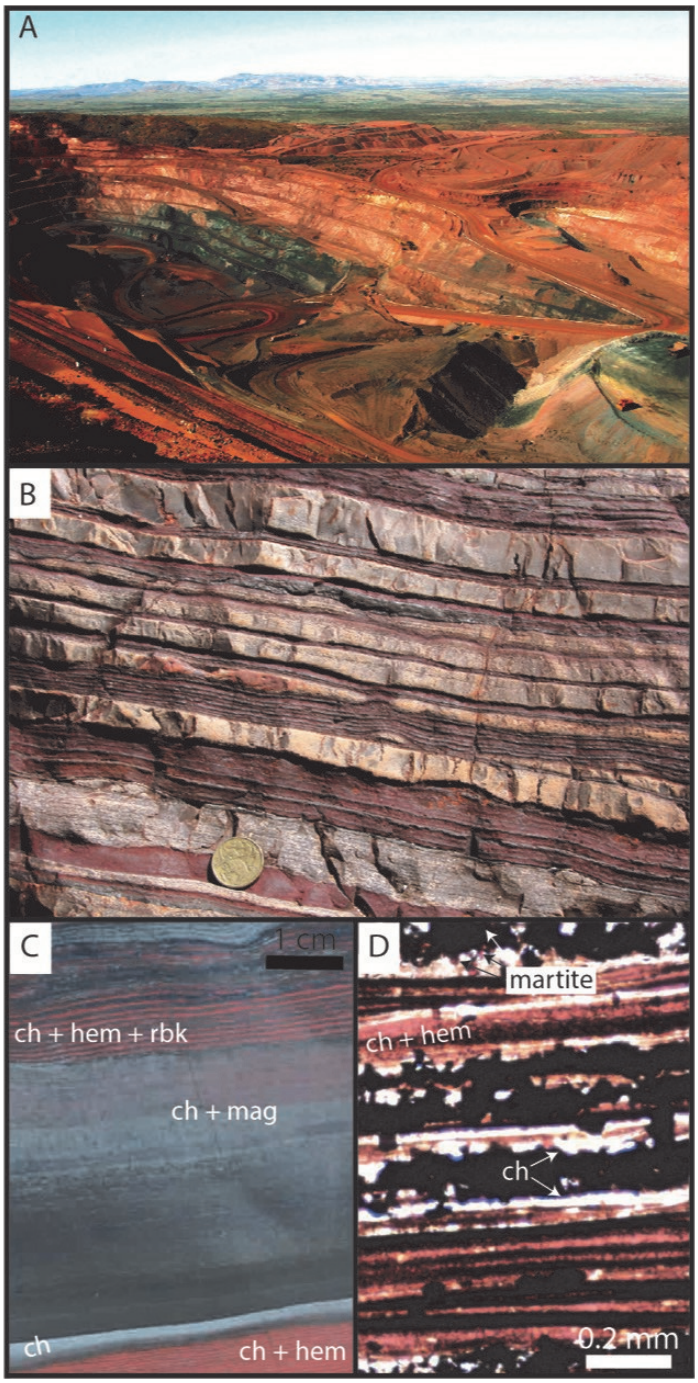

Figure 1. Representative images of Paleoproterozoic iron formations (IF). (A) Aerial overview of the 2.48 Ga Dales Gorge Member along the southern ridge at Tom Price, Western Australia. Photo credit: Mark Barley. (B) Section of banding in the 2.45 Ga Joffre Member, Western Australia. (C) This core from the Joffre Member displays pale grey micro- and mesobands of alternating chert and magnetite, dark grey magnetite mesobands and reddish and bluish (1 mm thin) microbands of chert–hematite–riebeckite. (D) Coarse- and fine-grained magnetite microbands with chert and very fine hematite. The latter likely is a product of secondary magnetite oxidation. Note the single grains of martite upper left. ch = chert, hem = hematite, mag = magnetite, rbk = riebeckite.

(1993), the authors proposed that as a result of global ice cover, dissolved Fe(II) built up in concentration within the water column, and then during glacial melting, seawater became exposed to O_2 leading to Fe(II) oxidation. Lechte and Wallace (2016) also proposed that some of those IF were deposited below the ice shelf through an ice pump mechanism where cold oxygenated glacial fluids mixed with ferruginous seawater.

For the purposes of discussing IF in the context of Earth's oxygenation, we focus below only on Superior-type IFs.

One of their notable characteristics is alternating iron-rich and silica-rich layers (Fig. 1B) which give the sediments the name banded iron formation (BIF). The layers range from macrobands (metre-thick) to the mesobands (centimetre-thick) by which they are typically defined to microbands (millimetre and sub-millimetre layers; Fig. 1C-D). The latter have been linked to episodic hydrothermal input and hypothesized to represent an annual depositional process (e.g. Trendall and Blockley 1970; Morris 1993) driven by the metabolic activity of microbial plankton (Posth et al. 2008; Schad et al. 2019a). There is, however, another Superior-type iron formation called granular iron formation (GIF). What differentiates GIF from BIF is that the former was deposited in a coastal marine environment subject to riverine input of clastic sediment (i.e. mud, silt and sand). Many of the granules appear to have been derived by sedimentary re-working of iron-rich clay, mudstone, arenite, and even stromatolites (e.g. Simonson and Goode 1989), while others are composed of concentric cortices of hematite that were likely precipitated where Fe(II)-rich waters met more oxygenated shallow seawater (e.g. Dorland 1999). By contrast, BIF typically lack evidence of wave action. For simplicity, we will from herein simply use the abbreviation IF.

The iron-rich layers of IF consist of minerals such as hematite (Fe_2O_3), magnetite (Fe_3O_4), iron-bearing carbonate minerals like siderite ($FeCO_3$) and dolomite–ankerite ($(Ca,Mg)CO_3$ or $Ca(Fe,Mg,Mn)(CO_3)_2$), as well as various Fe(II)–/Fe(III)-silicates. In contrast, the silica-rich layers are mainly comprised of microcrystalline silica (Klein 2005). It is widely recognized that none of the minerals observed in IF are of primary origin, indicating that the minerals initially deposited on the seafloor did not endure. Instead, the mineral assemblages observed in IF today are the result of multiple post-depositional alteration events that occurred during diagenesis (low-temperature transformations during burial in sedimentary basins) and metamorphism (high-temperature changes induced by deep burial as well as tectonic and magmatic events). Additionally, research has shown that the mineral compositions preserved in IF differ along a gradient from deeper water settings near hydrothermal sources of Fe(II) to more distal, shallower environments. For instance, in the Mesoarchean Witwatersrand IF in South Africa, this variation manifests as a transition from hematite-dominated facies in the most distal settings to magnetite and siderite proximal to the paleoshore. This transition reflects an increasing input of organic matter that facilitated the diagenetic and metamorphic reduction of Fe(III) (Smith et al. 2013).

The iron oxides found in IF are believed to have originated from an initial ferric oxyhydroxide phase, such as ferrihydrite ($Fe(OH)_3$). This phase was biologically precipitated from seawater in the well lit upper layers of the ocean. Precipitation occurred through the oxidation of dissolved ferrous iron (Fe^{2+}), with concentrations estimated to range from 0.03 to 0.5 millimolar (mM) (Holland 1973; Morris 1993), although concentrations exceeding 1.0 mM have also been proposed (Derry 2015; Jiang and Tosca 2019). Recent research suggests that in the presence of dissolved silica, which could have reached concentrations as high as 2 mM during the Archean eon (Siever 1992; Maliva et al. 2005), the initial precipitate in the water column could have been a gel-like substance composed of ferric oxyhydroxide and silica (Konhauser et al. 2007a; Fischer and Knoll 2009; Percak-Dennett et al. 2011).

Conversely, the mineral greenalite ($Fe_3Si_2O_5(OH)_4$) has been identified in several IF and interpreted as a relict primary mineral phase formed in the ancient water column (Rasmussen et al. 2017, 2021a; Johnston et al. 2018). Initially, greenalite was proposed by Konhauser et al. (2007b) as a primary precipitate in the ancient oceans, but crucially having formed below the photic zone in deep (> 100 m) waters and thus in the absence of an oxidant such as light or O_2. Such an interpretation would be consistent with greenalite nanoparticles forming during hydrothermal venting in environments that were distal to the deposition of Superior-type IF (e.g. Tosca and Tutolo 2023). By contrast, in the photic zone, ferrihydrite would have formed. The controversy over whether ferrihydrite versus greenalite was the primary precipitate then comes down to whether one thinks that there was a photosynthetic component to the marine biosphere at that time. From our perspective, in the run up to the Great Oxidation Event (GOE), the shallow marine environments were already colonized, with a diverse marine biota including cyanobacteria and underlying anoxygenic phototrophs (Schad et al. 2019b). Archean IF also exhibit a wide range of iron isotope ratios that cannot be explained by small isotopic effects resulting from direct seawater precipitation of iron silicates like greenalite (e.g. Planavsky et al. 2012a; Smith et al. 2017; Albut et al. 2019). Moreover, the transformation of greenalite into hematite requires either a carbonation reaction to siderite that then thermally decomposes to hematite (Rasmussen and Muhling 2018) or extensive sediment oxidation by secondary O_2-rich fluids (Rasmussen et al. 2014; Rasmussen and Muhling 2020). Recent hydrological modelling, however, suggests that such 'supergene' processes were not widespread throughout the IF record (Robbins et al. 2019b). In summary, there is compelling evidence indicating that Fe(II) silicate minerals were not the predominant water-column precipitates in the mass balance of IF, although they likely did precipitate in deeper, Fe(II)-rich seawater, e.g. seaward of the continental shelf.

The precipitation of Fe(III) occurred at the boundary between reduced upwelling waters rich in Fe(II) and the waters of the sunlit upper layer of the ocean (see Fig. 2). Three biological oxidation mechanisms have been proposed to explain this process: anoxygenic Fe(II)-based photoautotrophy, also

https://doi.org/10.12789/geocanj.2023.50.201

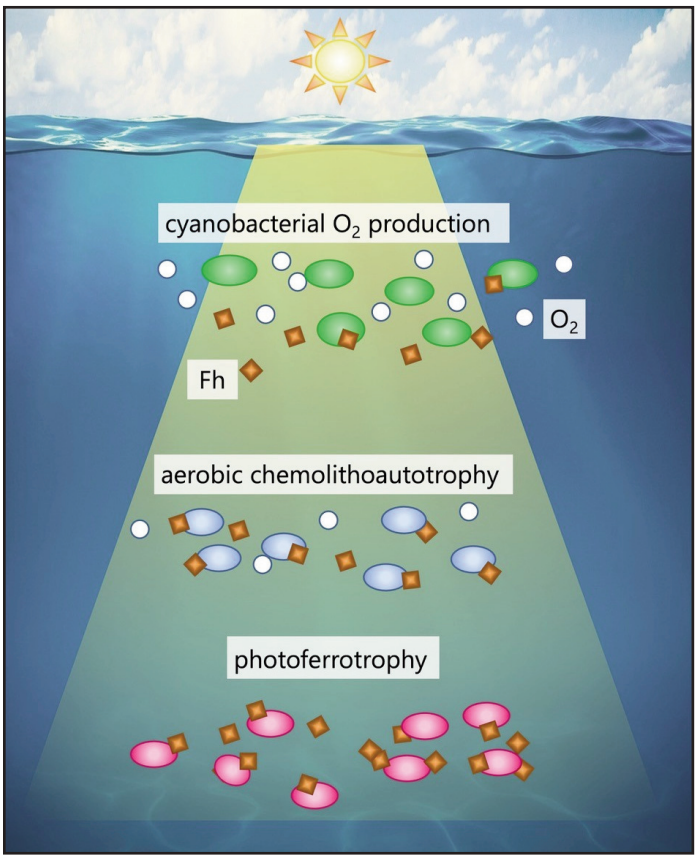

Figure 2. Three mechanisms of biological Fe(II) oxidation in the Precambrian oceans. (Top) reaction of cyanobacterially generated O_2 with dissolved Fe(II); (middle) oxidation via chemolithoautotrophic Fe(II) oxidizing bacteria that grow under low O_2 concentrations; and (bottom) direct oxidation via Fe(II)-based anoxygenic photosynthesis (photoferrotrophy) below the redoxcline where there is no free O_2. Fh = ferrihydrite.

known as photoferrotrophy (reaction 1); aerobic chemolithoautotrophy with O_2 produced by oxygenic photosynthesis (reactions 2a-b); and abiotic oxidation via O_2 from oxygenic photoautotrophy (reaction 3).

[1] $24Fe^{2+} + 6CO_2 + 66H_2O \rightarrow 24Fe(OH)_3 + C_6H_{12}O_6 + 48H^+$
[2a] $6H_2O + 6CO_2 \rightarrow C_6H_{12}O_6 + 6O_2$
[2b] $36Fe^{2+} + 3O_2 + 6CO_2 + 96H_2O \rightarrow C_6H_{12}O_6 + 36Fe(OH)_3 + 72H^+$
[3] $4Fe^{2+} + O_2 + 10H_2O \rightarrow 4Fe(OH)_3 + 8H^+$

Among the three biological mechanisms, photoferrotrophy is considered to be the most ancient (Hartman 1984; Widdel et al. 1993). Positive iron isotope fractionations, thought to represent a primary oxidative process operating under low O_2 availability, are observed in the approximately 3.78 Ga IF of the Isua Supracrustal Belt in Greenland and suggest the presence of photoferrotrophs in the Eoarchean seawater (Czaja et al. 2013). While it is generally agreed that cyanobacteria evolved before the onset of the GOE around 2.5 billion years ago, the exact timing of their emergence remains uncertain (e.g. Planavsky et al. 2021). Sustainable concentrations of O_2 in the ancient oceans are also not well established, with estimates ranging from very low levels in the Archean, on the order of a few nanomolar (nM) (Olson et al. 2013), to higher concentrations of up to 100 micromolar (mM) in the water column at a few hundred metres depth (Kendall et al. 2010). Under low O_2 conditions, aerobic chemolithoautotrophic species could have exploited the slow abiotic oxidation of Fe(II) (e.g. Søgaard et al. 2000) which were encountered just above the redoxcline in the ancient water column (Chan et al. 2016). As the oceans became more oxygenated, abiotic oxidation of Fe(II) (as described in reaction 3) likely became the primary mechanism for ferrihydrite precipitation, following the classic model proposed by Cloud (1965).

Several arguments favour a dominant role for photoferrotrophs before the GOE. First, they would have had a competitive advantage over early cyanobacteria, as they were better adapted to benefit from upwelling phosphorus-rich deep waters, thanks to their ability to grow under low-light conditions (Kappler et al. 2005). Cyanobacteria, on the other hand, have higher phosphorus requirements (Jones et al. 2015; Schad et al. 2019a). Second, the photoferrotrophs had first access to dissolved Fe(II) which is their electron donor, and even in modern ferruginous environments, such as Lake Matano in Indonesia, photoferrotroph activity controls dissolved Fe(II) concentrations in the water column (Crowe et al. 2008). Third, the ferruginous conditions associated with IF deposition may have been toxic to cyanobacteria (Swanner et al. 2015). In all likelihood, the relative roles of each metabolism varied in space and time, depending on nutrient availability and the influence of hydrothermal water inputs (Beukes and Gutzmer 2008). Determining the relative contributions of photoferrotrophs and cyanobacteria to IF deposition is an ongoing area of research (Konhauser et al. 2018).

The oxidation of dissolved Fe(II) would produce biomass that settled to the seafloor together with the Fe(III) minerals (e.g. Konhauser et al. 2002, 2005; Li et al. 2011; Posth et al. 2013a, b). If, as today, the organic carbon (C_{org}) was oxidized during burial by either diagenesis or metamorphism, the relevant question is which terminal electron acceptor was present at the seafloor during times of IF deposition, and at what concentrations? Despite the possibility of some oxic surface waters being generated by cyanobacterial activity as early as 3.0 Ga (e.g. Planavsky et al. 2014), deep waters, and by extension the seafloor, remained anoxic unlike today where sediment pore waters can have dissolved O_2 at depths of several millimetres, and locally even greater depths (Konhauser 2007). In the absence of O_2, the fermentation products in the bottom waters and/or shallow sediment would have been oxidized via some other anaerobic respiratory process. The paucity of O_2 would also have meant minimal nitrate (NO_3^-), manganese oxide (MnO_2) and sulphate (SO_4^{2-}) availability (Fig. 3A). By contrast, the ferric minerals in the primary IF sediment would have been favourable electron acceptors for the oxidation of organic matter (Walker 1984; Nealson and Myers 1990) through the process of dissimilatory iron reduction (DIR) by various bacteria (reaction 4). Significantly, coupling the reduction of some Fe(III) minerals to the oxidation of organic matter not only explains the low content of C_{org} in IF (< 0.5 wt.%; Gole and Klein 1981), but it also explains highly negative $\delta^{13}C$

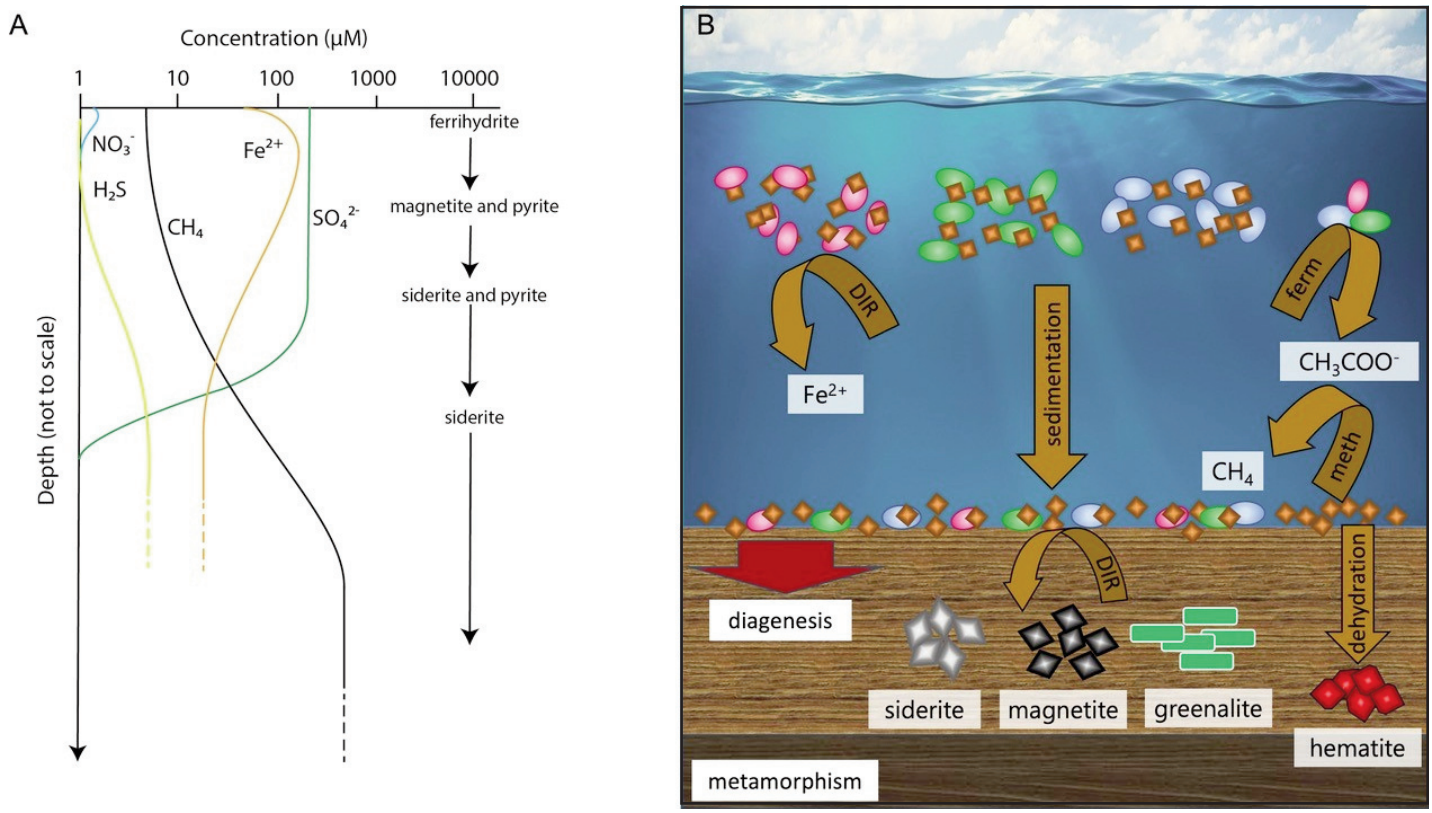

Figure 3. (A) Plausible Archean pore water profile during early diagenesis wherein minerals on right-hand side are dominant controls on pore water Fe speciation. (B) Schematic showing changes to the initial ferrihydrite and biomass associated with burial (diagenesis and metamorphism). After sedimentation, metabolically driven redox processes by fermenters and dissimilatory iron reducing microorganisms (DIRM) take place, possibly also involving methanogens. Pressure and temperature alter the source sediment and cause mineral overprinting. If biomass is present, DIR can lead to magnetite, siderite and greenalite precipitation, while in organic-lean sediments, ferrihydrite dehydrates to hematite. ferm = fermentation; meth = methanogenesis.

values of the early diagenetic Fe(II)–rich carbonate deposits (Baur et al. 1985; Craddock and Dauphas 2011), the highly negative δ^{56}Fe values in magnetite-rich IF (Johnson et al. 2008; Heimann et al. 2010), and the small-scale heterogeneity in δ^{56}Fe values between alternating IF bands (e.g. Steinhoefel et al. 2010). In sum, the negative δ^{13}C values indicate that organic matter was an important source of the C incorporated into the carbonate minerals, the negative δ^{56}Fe in magnetite indicates DIR, while the heterogeneity likely suggests variable degrees of partial Fe(II) oxidation in surface waters, precipitation of different mineral phases and/or post-depositional Fe redistribution but not wholescale overprinting by secondary fluids. Moreover, it explains the presence of Fe(II)-bearing minerals in IF (Fig. 3B): (1) magnetite or iron carbonate when the remineralization of buried organic matter was coupled to Fe(III) reduction (reactions 5 and 6), either during diagenesis or metamorphism (Köhler et al. 2013; Li et al. 2013; Halama et al. 2016); (2) hematite (reaction 7), through dewatering and silica release, when C_{org} was insufficient for complete Fe(III) reduction (Sun et al. 2015); and (3) iron silicate phases, such as greenalite (reaction 8), when silica sorbed onto ferric oxyhydroxides reacted with other cationic species during Fe(III) reduction within sediment pore waters (e.g. Morris 1993; Fischer and Knoll 2009).

[4] $8Fe(OH)_3 + CH_3COO^- \rightarrow 8Fe^{2+} + 2HCO_3^- + 15OH^- + 5H_2O$
[5] $2Fe(OH)_3 + Fe^{2+} \rightarrow Fe_3O_4$ (magnetite) $+ 2H_2O + 2H^+$
[6] $Fe^{2+} + HCO_3^- \rightarrow FeCO_3$ (siderite) $+ H^+$
[7] $2Fe(OH)_3 \rightarrow Fe_2O_3$ (hematite) $+ 3H_2O$
[8] $3Fe^{2+} + 2Si(OH)_4 + H_2O \rightarrow Fe_3Si_2O_5(OH)_4$ (greenalite) $+ 6H^+$

Recent experimental work also supports the possibility that the formation of ferrous silicate mineral phases may be the result of DIR (Nims and Johnson 2022). Finally, ferrous iron sorption to these particles may also have given rise to 'green rust'-type deposits that eventually transformed into magnetite or iron silicate minerals (Halevy et al. 2017; Li et al. 2017).

Although much of the discussion on DIR in IF has focused on processes within the sediment, it is also likely that Fe(III) reduction occurred in the water column. To test this possibility, Konhauser et al. (2005) modelled the ancient Fe cycle based simply on conservative experimental rates of photosynthetic Fe(II) oxidation in the photic zone. They showed that under ideal growth conditions, as much as 70% of the biologically produced Fe(III) could have been recycled back into the water column via fermentation and C_{org} oxidation coupled to DIR. By comparing the potential size of biomass generated phototrophically with the reducing equivalents required for Fe(III) reduction and magnetite formation, they also hypothe-

https://doi.org/10.12789/geocanj.2023.50.201

sized that another anaerobic metabolic pathway might have been utilized in the surface sediment or water column to oxidize C_{org}, specifically a consortium of fermenters and methanogens (Konhauser et al. 2005). Interestingly, at Lake Matano, Crowe et al. (2011) demonstrated that more than 50% of organic matter formed in the water column is degraded through methanogenesis, despite high abundances of ferric oxyhydroxides in the lake sediment.

Even though biomass degradation underpins the conversion of primary IF sediment into the rocks we observe today, our understanding of the complex feedback loops between these microbial processes remains poorly resolved. A recent study by Schad et al. (2022) provided a first attempt to ascertain the interdependent effects of these microbial processes. Those authors co-cultivated photoferrotrophs and dissimilatory Fe(III)-reducing bacteria (DIRB) and observed that both metabolic processes can be coupled, where DIR reduced the cell-Fe(III) mineral aggregates formed by photoferrotrophs and the latter re-oxidized the Fe(II) formed by the DIRB. Crucially, however, their experiments required lactate to be added as C_{org} source and electron donor for the DIRB. This is not surprising given that many anaerobic heterotrophs cannot directly utilize complex organic compounds as their C_{org} source and electron donors but instead rely on fermentative bacteria to produce simple organic compounds such as hydrogen gas (H_2), lactate, or acetate (reaction 9; Rico et al. 2023; Mahmoudi et al. 2023). Consequently, what remains unknown is if the biomass formed by the photoferrotrophs during the initial primary production would in due course become available for DIRB or other downstream microbial processes such as methanogenesis (Konhauser et al. 2005).

[9] $C_6H_{12}O_6 + 2H_2O \rightarrow 2CH_3COO^-$ (acetate) $+ 2CO_2 + 4H_2 + 2H^+$

WHY IRON FORMATIONS ARE USEFUL AS ANCIENT SEAWATER PALEOPROXIES

It has often been argued that IF are deep water sediments due to the lack of current- and wave-generated structures. This is true, but one needs to consider that storm wave base is typically < 50 m (Immenhauser 2009), although waves reaching greater depths do occur (e.g. Peters and Loss 2012). Thus, most IF precipitation would have occurred on the continental shelf (Fig. 4), which today averages 130 m (Tyson and Pearson 1991). For comparison, sea level is believed to have shown an approximately 400 m range of variation over geological time (Trendall 2002). Moreover, the preservation of IF in the rock record argues against their deposition on a subducting deep seafloor. On the landward side, IF are often juxtaposed against either siliciclastic or carbonate sediments, and with minor amounts of volcanic rocks (Gross 1980). They typically formed in open-marine environments during high sea level (e.g. Simonson and Hassler 1996). The presence of siliciclastic sediment depended upon riverine input, and it is not uncommon to find IF interbedded with shale. Often that shale is also organic rich (i.e. black shale) which indicates the addition of planktonic biomass to the clastic sediment (Bekker et al. 2010). Interestingly, experimental studies using photoferrotrophs and cyanobacteria to precipitate ferrihydrite have shown that some cells aggregate with the ferrihydrite (e.g. Posth et al. 2010; Li et al. 2021), whereas other cells have the propensity to remain unmineralized, especially in the presence of dissolved silica (e.g. Gauger et al. 2016; Schad et al. 2019b). The latter could have led to the large-scale deposition of IF lean in organic matter, which in turn, facilitated the deposition in coastal sediments of organic-rich shale that fueled microbial methanogenesis (Thompson et al. 2019).

As authigenic chemical sediments, IF effectively captured the evolving elemental and isotopic signatures of marginal marine seawater, and in this regard, my research group and collaborators have pioneered their exploitation for better understanding Earth's transition to an oxygenated planet. The utility of IF is based on several assumptions and conditions. First, evidence supporting the idea that IF record authigenic marine signatures includes marine-like rare earth element and yttrium (REE+Y) patterns and small-scale chemical variations that argue for the preservation of environmental signals (e.g. Bau and Möller 1993; Bau and Dulski 1996; Bolhar et al. 2004; Alexander et al. 2008; Pecoits et al. 2009; Haugaard et al. 2013; Robbins et al. 2019a). A concern potentially compromising the IF record is the possibility of post-depositional mobilization of trace elements, which can overprint or even eradicate authigenic marine signatures. However, limited post-depositional mobilization or addition of trace elements in IF is indicated by systematic REE and Fe isotope variations, both within and between Fe-rich mesobands despite experiencing diagenetic and metamorphic conditions up to amphibolite facies (e.g. Frost et al. 2007; Whitehouse and Fedo 2007; Steinhoefel et al. 2010). In fact, trace element compilation efforts for IF have often limited their scope to samples falling at greenschist facies or less to provide the most robust estimates possible of trace element abundances. Second, ferrihydrite, the likely precursor phase for hematite and magnetite in IF, can faithfully preserve the elemental and isotopic compositions of seawater, as has been demonstrated through ferrihydrite adsorption and diagenesis experiments (e.g. Døssing et al. 2011; Robbins et al. 2015; but see also Halevy et al. 2017 for a different view). Third, this seawater signal is commonly uncontaminated by continentally derived detrital materials, given that BIF (versus GIF) generally contain very low levels of detrital tracer elements such as aluminum (Al) and titanium (Ti) (Holland 1978). Collectively, this means that IF geochemical data often provide a purely 'authigenic' record of marine chemistry.

The chemical signals archived in 'BIF' can be harnessed by leveraging the predictable behaviour of adsorption reactions that take place on the surface of authigenic ferrihydrite. These ferrihydrite minerals were initially formed from, and reached equilibrium with, the surrounding seawater during their precipitation. In natural environments, where trace elements are captured and stored by ferrihydrite through a combination of adsorption and co-precipitation reactions, simplified distribution coefficient models can be employed to establish an empirical relationship between the concentration of an element in the precipitate and the dissolved concentration at the time of precipitation. This predictive characteristic of ferrihydrite

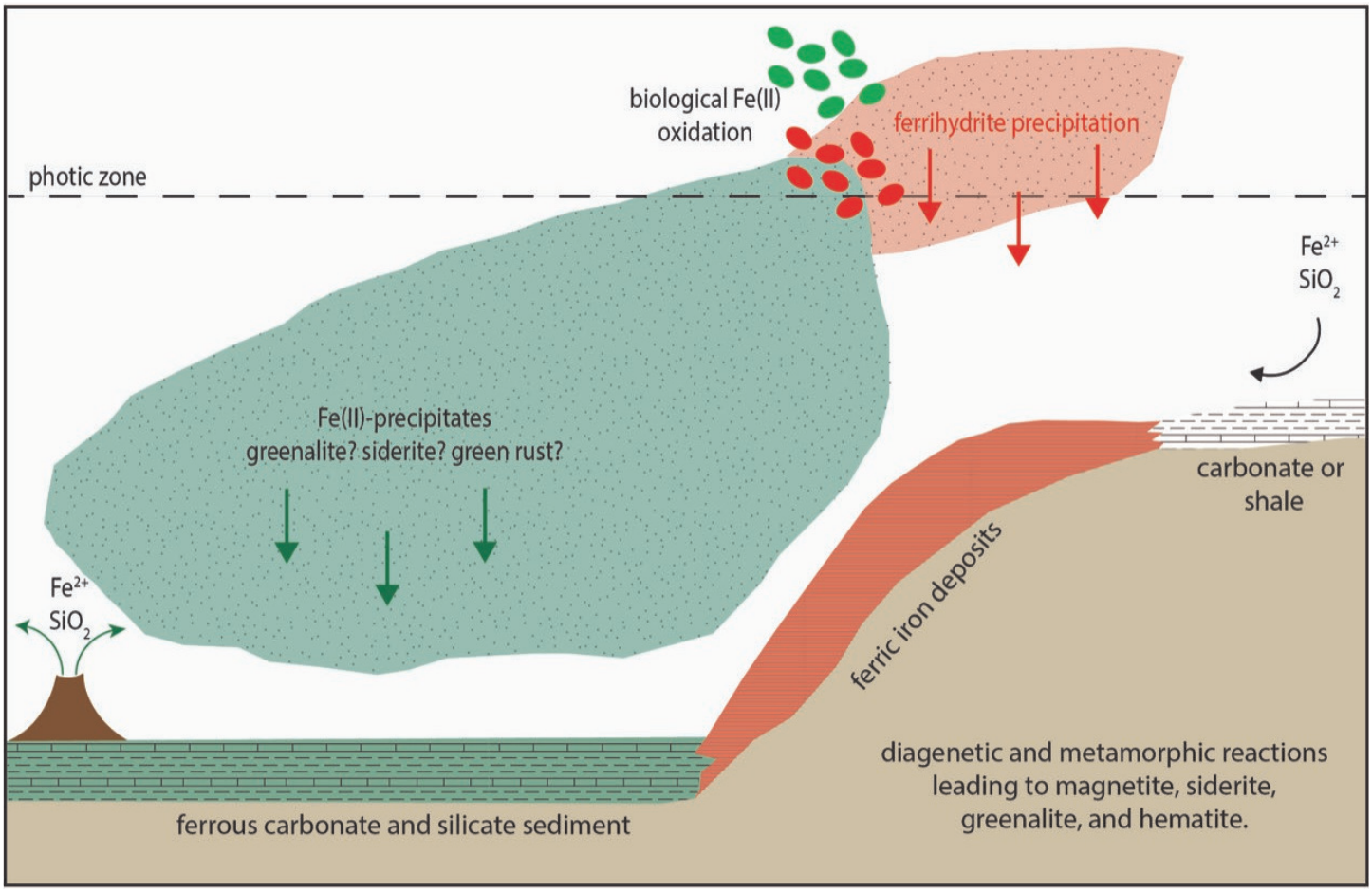

Figure 4. Cross-section of deep submarine source of dissolved Fe(II) that upwells onto the continental shelf where biological Fe(II) oxidation takes place. This leads to the precipitation of ferrihydrite as the precursor sediment for iron formations (IF). Some of ferrihydrite was later reduced through direct bacterial Fe(III) reduction by dissimilatory iron reduction utilizing organic carbon (biomass) as the electron donor. In the absence of a Fe(II) oxidant, the direct precipitation of greenalite or siderite may have taken place in the pelagic water column and continental slope. Along the coast either siliciclastic or carbonate sediments were deposited depending on the presence or absence of riverine input, respectively.

sorption reactions has been used to gain a deeper understanding of the IF record. Specifically, it provides insights into the limitations that Precambrian primary productivity may have faced, whether by the sequestration of bio-essential nutrients by the ferrihydrite itself, or its record of nutrient limitations driven by other factors such as different styles of volcanism, continental weathering, or even internal oceanic cycling (Robbins et al. 2016).

One alternative method for assessing ancient marine trace element concentrations in IF data, without relying on experimentally derived partition coefficients, involves analyzing the relationship between specific trace elements and iron within the IF record itself. Taking nickel (Ni) as an example, there is a clear correlation between the deposition of Fe and Ni. As Fe increases, Ni also increases, consistent with the expected behaviour of Ni sorption to ferrihydrite governed by partition coefficients. By plotting these variables on a graph, we can also overlay the scaling anticipated between a trace metal and Fe based on proposed partitioning scenarios (cf. Robbins et al. 2013; Konhauser et al. 2015). The advantage of this approach is that the hypothesized partitioning scenarios can be compared with the actual data from the IF record. If the proposed scenarios accurately represent the deposition of IF minerals, the lines representing these scenarios should encompass most of the IF data. In fact, when the K_D (distribution coefficient) values predicted by Konhauser et al. (2009) are superimposed on the graph (Fig. 5), nearly all the Ni/Fe values observed in the IF record fall within the predicted ranges. It is important to note that this agreement does not confirm the accuracy or validity of experimentally determined K_D values. The slope in the solid-phase Ni versus Fe space is calculated as $K_D*[Ni]_{sw}$ and is equally influenced by $[Ni]_{sw}$ (dissolved concentration of Ni in seawater). In the case of the partitioning scenarios proposed by Konhauser et al. (2009), $[Ni]_{sw}$ values were originally extrapolated from data in the rock record using experimentally determined K_D values. Therefore, the presented $K_D*[Ni]_{sw}$ scenarios (slopes in Ni versus Fe space) are tuned to this specific dataset, and the apparent correspondence may be considered circular. However, Figure 5 demonstrates two key points: (1) partitioning scenarios can be readily evaluated against rock record data to establish their plausibility, and (2) in future investigations, supposed free parameters (K_D, $[Ni]_{sw}$) could

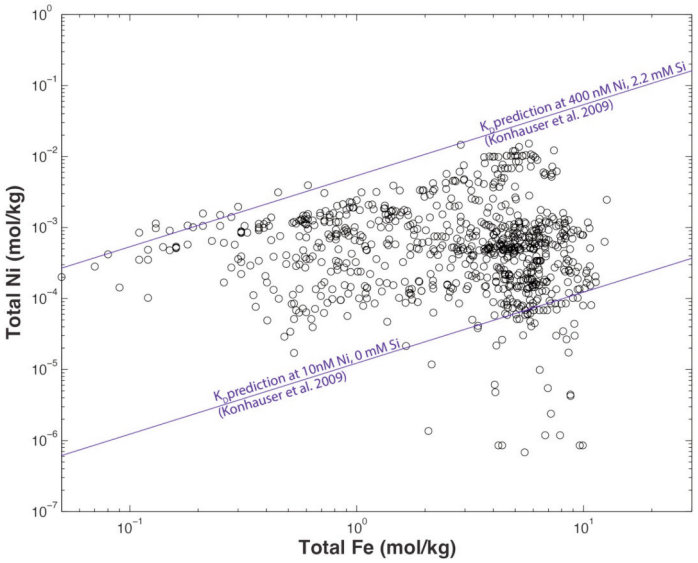

Figure 5. The scaling of Ni with Fe as recorded in the iron formations (IF) record. Superimposed on the IF data are the proposed partitioning scenarios of Konhauser et al. (2009). Note that almost all IF data are constrained by the lines representing the high silica, high Ni and low Si, low Ni partitioning scenarios. Cross plots such as these allow for proposed partitioning scenarios to be tested against IF data. Adapted from Konhauser et al. (2015).

potentially be adjusted based on rock record data to explore feasible scenarios in the K_D–$[Ni]_{sw}$ space. This approach was employed by Robbins et al. (2013) for zinc (Zn)/Fe when experimentally determined partition coefficients were not available.

It is important to note that while the K_D approach, when combined with rock record data, yields what may be considered quantitative constraints on ancient seawater composition, this approach is not without its limitations. Strictly speaking, K_D values are empirical relationships that describe the experimental system being considered. Their subsequent extrapolation to different conditions (pH, ionic strength, etc.) is therefore somewhat tenuous. However, they provide a relatively simple and effective method for generating first-order constraints on the composition of ancient seawater billions of years ago, and therein lies their true utility.

TRACE ELEMENT TEMPORAL TRENDS IN IRON FORMATIONS

In much of the modern Earth's oceans, microbial life has an abundance of C, nitrogen (N), and O_2. However, the scarcity of essential trace nutrients such as phosphorus (P), cobalt (Co), manganese (Mn), molybdenum (Mo), Ni, vanadium (V), and Zn limits primary production (e.g. Morel and Price 2003; Sunda 2012). This limitation has likely existed since the emergence of life over 3.8 Ga, when microbes began developing intricate strategies to scavenge metals and incorporate them from their aqueous surroundings. The availability of trace nutrients in seawater is influenced by long-term geological processes, including the gradual cooling of the upper mantle, changes in volcanic activity and continental composition, and the intermittent accumulation of atmospheric O_2, which facilitated oxidative weathering reactions. The notion that these events may have played a role in directing microbial evolution at the enzymatic level over billions of years is a relatively recent but profound concept (see Anbar and Knoll 2002). This is because microbial evolutionary innovations ultimately influenced the habitability of Earth for the more complex organisms that emerged later. In this context, we will explore how IF have been used to understand the composition of seawater for three trace elements in deep geological time. The primary objective is to gain a better understanding of the co-evolution of the Precambrian environment and biosphere and especially as it relates to atmospheric oxygenation.

Phosphorus

Throughout Earth's history, P has been the primary element limiting global marine primary production on geologic timescales (Tyrrell 1999; Kipp and Stüeken 2017; Reinhard et al. 2017; Laakso and Schrag 2018; Hao et al. 2020). Marine phytoplankton likely emerged during the Archean eon, making it crucial to understand the availability of dissolved phosphorus (P_d) to gain insights into the early evolution of the marine biosphere. In present day surface waters of the oceans, P_d is typically found as protonated inorganic phosphate species (e.g. HPO_4^{2-}), with an average global ocean concentration of approximately 2.3 μM (Levitus et al. 1993; Bruland et al. 2014). However, the range of P_d concentrations in the Neoarchean and early Paleoproterozoic (2.8–2.0 Ga) oceans, spanning the GOE, remains unresolved.

Several studies have been conducted to reconstruct paleomarine phosphorus concentrations by examining the ratios of phosphorus to iron (P/Fe) in IF (Bjerrum and Canfield 2002; Konhauser et al. 2007a; Planavsky et al. 2010; Jones et al. 2015). These studies were based on the understanding that the phosphorus content in modern marine hydrothermal plume ferric oxyhydroxide precipitates (such as ferrihydrite) can be used to establish an empirical relationship between seawater P_d and the ratio of solid-phase phosphorus to iron (P_s/Fe_s) in the ferric oxyhydroxide precipitates (Feely et al. 1998). This relationship exists because the precipitated ferric oxyhydroxides have a strong affinity for phosphorus. The relationship is quantified by a linear distribution coefficient where

$$K_D = \frac{P_s/Fe_s}{P_d}.$$

Building upon this relationship, Bjerrum and Canfield (2002) investigated the IF record to estimate ancient seawater P_d and found that during the Archean P_d averaged 0.15 μM (ranging from 0.03 to 0.29 μM), which corresponds to approximately 10–25% of present-day levels. The authors argued that IF served as a significant sink for P, resulting in a P crisis. This finding was noteworthy because it resolved a paradox that existed then. While a number of studies on the genomes of modern cyanobacteria (e.g. Sánchez-Baracaldo et al. 2022), geochemical indicators for free O_2 (e.g. Planavsky et al. 2014), and fossilized microbialites (Homann et al. 2015) all suggested the potential evolution of cyanobacteria before 3.0 Ga, based on the rock record it is widely accepted that permanent atmos-

pheric oxygenation (i.e. the GOE) did not occur until after 2.5 Ga (e.g. Ostrander et al. 2021). Consequently, the question arose: why did it take so long for O_2 to accumulate in the atmosphere? The Bjerrum and Canfield study pointed towards nutrient limitation as a potential factor.

However, when using P_s/Fe_s ratios as a paleo-proxy, it is crucial to consider the evolution of the silicon (Si) cycle and dissolved silica concentrations (Si_d; H_4SiO_4) due to the inverse relationship between the K_D value for phosphate–ferrihydrite sorption and Si_d, caused by the competitive adsorption of aqueous silica species (Konhauser et al. 2007a). Modern seawater typically has Si_d concentrations below 0.1 mM (Tréguer et al. 1995), while Si_d concentrations during much of the Precambrian may have been saturated with respect to amorphous silica (2.2 mM) (Siever 1992). Such significant differences in Si_d can result in substantial changes to the K_D value for P adsorption onto ferric oxyhydroxide. Indeed, Konhauser et al. (2007a) demonstrated that ferrihydrite precipitation in the presence of high Si concentrations, which leads to Si-rich ferrihydrite (Reddy et al. 2016; Zheng et al. 2016), adsorbs less P compared to ferrihydrite formed under low Si concentrations. As a result, estimated P_d values for the Archean were calculated to be as high as 5.25 ± 2.63 μM. Subsequently, Planavsky et al. (2010) combined the partitioning coefficients derived by Konhauser et al. (2007a) with P/Fe ratios in the IF record and suggested that P levels in the Precambrian oceans were at least as high as modern seawater, and possibly even higher. Jones et al. (2015) subsequently conducted similar partitioning coefficient experiments but included Mg^{2+} and Ca^{2+} in the experimental solutions to better approximate seawater composition. This subtle difference in experimental conditions resulted in estimated Archean P_d concentrations ranging from 0.04–0.13 μM. These examples highlight the susceptibility of P_d estimates to variability in the proposed K_D values. This may be an area of future research that could benefit from the application of more robust, thermodynamically grounded surface complexation models that can be iteratively tested to identify the ways in which accessory cations or anions affect partitioning of biologically critical elements such as P.

Using a different approach, Rasmussen et al. (2021b) reported the ubiquitous presence of nanometre-sized apatite crystals in IF dating between 3.46 to 2.46 Ga. The apatite is uniformly distributed within greenalite-rich layers. The authors subsequently argued that abundant greenalite precipitation in the open ocean led to high phosphate concentrations in seawater, perhaps approaching 100 μM. They argued that dissolved Fe^{2+} would have been limited by greenalite precipitation, thus inhibiting the formation of vivianite ($Fe_3[PO_4]_2 \bullet H_2O$), a potential deep sea phosphorus trap (Derry 2015). This work has support from experiments and models that show that Fe^{2+} significantly increases the solubility of phosphate minerals in anoxic systems, with possible P_d ranging from 200–400 μM (Brady et al. 2022).

Nickel

Nickel plays a crucial role in numerous prokaryotic metalloenzymes. It is essential for carbon reduction in both acetogenic and methanogenic bacteria and is a component of important cofactors such as methyl-coenzyme M reductase and acetyl-CoA synthase that are necessary for methane (CH_4) production (e.g. Hausinger 1987). Additionally, Ni is used in hydrogenases and carbon monoxide dehydrogenase, contributing to the reduction of CO_2 to CO and the production of acetyl-CoA (e.g. Ragsdale and Kumar 1996). In non-methanogenic organisms, Ni may be involved in urease activity and is also found in a superoxide dismutase present in various marine organisms, including planktonic cyanobacteria that may have evolved during the Neoproterozoic (Boden et al. 2021).

Initial estimates of dissolved Ni concentrations (Ni_d) in the early ocean were obtained through geochemical modelling (Saito et al. 2003) and microbial genomics (Zerkle et al. 2005). These studies suggested that seawater Ni_d was relatively consistent from the Archean to the present day. This presumed uniformity was mainly attributed to Ni behaving conservatively under various redox conditions in water. However, a compilation of Ni contents in IF over time (Konhauser et al. 2009) revealed a consistent and rapid decline in Ni_d around 2.7 Ga (Fig. 6A). This trend remained evident even after a near doubling of available IF data (Konhauser et al. 2015), indicating the observed decline in Ni within IF was a robust, first-order trend. By utilizing experimentally derived Ni partitioning coefficients for Si-rich ferrihydrite (considering elevated Si_d during the Precambrian), it was estimated that paleomarine Ni_d decreased by over 50% between 2.7 and 2.5 Ga, dropping from approximately 400 nM to 200 nM (Konhauser et al. 2009). This decline was attributed to mantle cooling, which led to a decrease in the frequency of Ni-rich ultramafic eruptions and subsequently limited the availability of Ni-source rocks susceptible to weathering. This trend was subsequently shown to have been captured in the sedimentary to early diagenetic pyrite record (Large et al. 2014) and recently been verified in an analysis of more than 96,000 continental volcanic rocks (Liu et al. 2021).

The decline in Ni_d would have had significant implications for microorganisms that relied on Ni, particularly CH_4-producing bacteria known as methanogens. These bacteria have a unique requirement for Ni in their CH_4-producing enzymes and have been implicated in regulating O_2 levels on ancient Earth. The CH_4 they produced reacted with O_2, keeping atmospheric levels of the latter low (Zahnle et al. 2006), although it can also at the same time contribute positively to atmospheric oxidation by promoting H_2 escape (Kasting et al. 2013). It is possible that a scarcity of Ni eventually triggered a cascade of events, starting with reduced CH_4 production, followed by the expansion of cyanobacteria into shallow-water habitats. In the end, this would have led to increased oxygenic photosynthesis and C_{org} burial, tipping the atmospheric balance in favour of O_2 and culminating in the GOE.

A study by Eickhoff et al. (2014) conducted a re-evaluation of the partitioning behaviour of Ni between biogenic and abiogenic ferrihydrite in the presence of silica. While the estimates presented by Eickhoff et al. (2014) cannot be directly compared to those of Konhauser et al. (2009) due to differences in their experimental approaches, their findings indicate

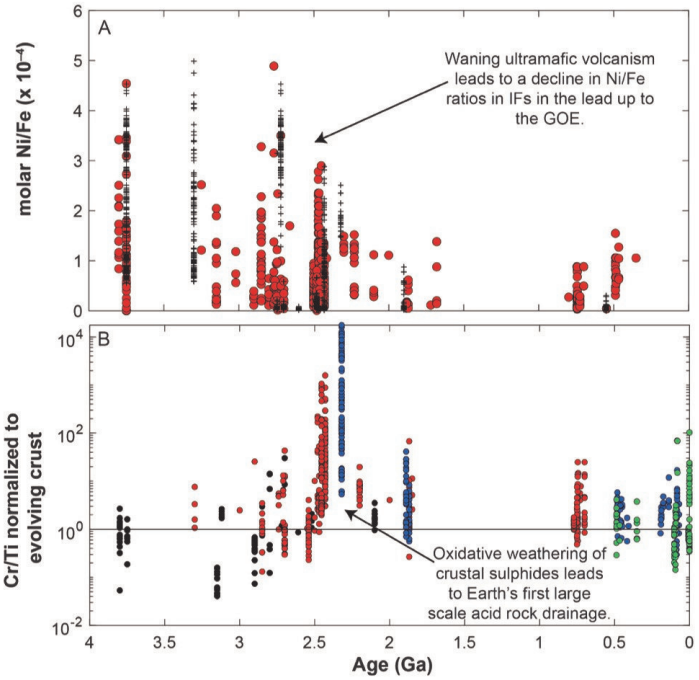

Figure 6. (A) Molar Ni/Fe ratios in iron formations (IF) adapted from Konhauser et al. (2015). Note red circles represent bulk analyses, with black + symbols representing laser ablation analyses; (B) molar Cr/Ti ratios in IF, normalized to evolving continental crust (Condie 1993). Symbols in (B) are black = Algoma-type IF; red = Superior-type IF; blue = granular iron formations and oolitic ironstones; green = Phanerozoic hydrothermal iron deposits. Adapted from Konhauser et al. (2011) and Hao et al. (2022). GOE = Great Oxidation Event.

that the presence of biomass leads to a decrease in Ni sorption onto ferrihydrite. Consequently, the estimates of paleomarine Ni_d based on IF may have been underestimated. This suggests that the decline in the paleomarine Ni reservoir, and the subsequent famine experienced by methanogenic bacteria, as described by Konhauser et al. (2009), might have occurred closer to the onset of the GOE.

Chromium

While chromium (Cr) has a limited biological role in most higher-level organisms, it is generally recognized as a toxin (Frausto da Silva and Williams 2001). Therefore, temporal patterns in seawater are unlikely to directly reflect evolutionary controls. Instead, studies in the sedimentary record have focused on analyzing Cr abundances and isotope compositions to track oxygenation in surface environments. The value of these investigations lies in the behaviour of reduced Cr, specifically Cr(III), which is immobile under neutral to alkaline pH conditions, but becomes mobile when either subjected to acidic conditions (Rai et al. 1989) or oxidized to Cr(VI) (Oze et al. 2007). Additionally, Cr stable isotopes are significantly fractionated during redox reactions (e.g. Ellis et al. 2002). Consequently, changes in Cr abundances and isotopic compositions are likely indicators of variations in the redox state of the oceans or atmosphere, as well as related shifts in Cr mobility mechanisms and sediment sources.

Based on the above understanding, Cr isotopes have been used to track the oxygenation of the atmosphere and oceans. In the case of 2.8–2.6 Ga IF, small variations in Cr isotope composition were initially proposed to represent short bursts of atmospheric O_2 that triggered the mobilization of Cr through oxidative weathering and its subsequent sequestration in IF prior to the GOE (Frei et al. 2009). The authors argued that the observed increases in δ^{53}Cr values ranging from +0.04 to +0.29‰ in IF at 2.7 Ga, and again at 1.8 Ga, resulted from the oxidation of Cr(III) to Cr(VI), with oxidation likely catalyzed by Mn(IV) oxides. Subsequently, Konhauser et al. (2011) examined the temporal trends in the degree of Cr enrichment in IF and found that the former was mostly immobile on land until approximately 2.48 Ga. However, within the subsequent 160 million years, during a period coinciding with independent evidence of oxygenation associated with the GOE, there were significant excursions in Cr abundances and Cr/Ti ratios, indicating an unprecedented scale of Cr solubilization (Fig. 6B) at a time when Cr isotope fractionation remained minimal, indicating that Cr was mobilized in Cr(III) rather than Cr(IV) form. The authors proposed that only the oxidation of a previously stable and abundant crustal pyrite reservoir by aerobic, chemolithoautotrophic Fe(II)-and S-oxidizing bacteria could have generated the necessary level of acidity to dissolve Cr(III) from ultramafic source rocks and residual soils. In other words, the emergence of novel microbial metabolisms coincided with atmospheric O_2 becoming available. During this period, muted δ^{53}Cr variations from –0.3 to +0.3‰ were interpreted as indicative of Cr cycling in its reduced form (Konhauser et al. 2011), in contrast to the highly variable values associated with ocean oxygenation during the Neoproterozoic (up to +4.9‰; Frei et al. 2009). This significant shift in weathering patterns, starting at 2.48 Ga, represents the earliest known example of acid rock drainage and persisted until the exposed crustal reservoir of pyrite was depleted, marking the end of an era characterized by intense chemical weathering on Earth.

To investigate earlier indications of photosynthetic O_2 production, researchers examined Cr isotope data from rocks in the Pongola Supergroup, South Africa. Crowe et al. (2013) discovered that the δ^{53}Cr isotope compositions of 2.96 Gyr old paleosols were fractionated compared to crustal values, suggesting the oxidative mobilization of Cr and the presence of low levels of atmospheric O_2 (~10^{-4} of present atmospheric levels, PAL). This O_2 level was necessary to oxidize Fe(II) to Fe(III) and thus prevent the ferrous iron from reducing Cr(VI) to Cr(III) during transport to the ocean. Interestingly, the analysis of roughly contemporaneous IF from the same region revealed δ^{53}Cr values up to 0.28‰. The authors proposed that the IF captured a mobile, δ^{53}Cr-enriched pool of Cr(VI) originating from oxidative weathering on the continents. This finding suggests the existence and activity of oxygenic photosynthesis approximately 500 million years prior to the GOE. The concept of early O_2 production is supported by the Mo isotope composition of the IF within the Pongola Supergroup, as the correlation between Mo isotope composition and Mn/Fe ratio indicates the presence of MnO_2 and its adsorption of isotopically light Mo during that period (Planavsky et al. 2014). However, it is also possible that the observed Cr isotope frac-

tionation in the 2.96 Ga paleosols, as reported by Crowe et al. (2013), is a result of localized O_2 production by cyanobacteria within a microbial mat (Lalonde and Konhauser 2015) or an artifact of modern weathering (Albut et al. 2018). In either scenario, the IF record of Cr, particularly in terms of its abundance and isotopic composition, offers valuable insights into O_2 production through photosynthesis, either in the early oceans or on land, and the associated oxidative weathering on the early continents. The early production of O_2 is consistent with recent genomic evidence for the emergence of oxygen producing or using enzymes (Jabłońska and Tawfik 2021) and sedimentological evidence including the observed relationship between Mo isotopes and Mn (Planavsky et al. 2014; Albut et al. 2018), Mn(IV) oxide deposition (Ossa Ossa et al. 2016; Robbins et al. 2023), and spatially resolved Mn enrichments that suggest a gradient from more reducing to oxidizing conditions that parallels the transition from deeper to shallower waters (Smith and Beukes 2023).

Evidence for environmental oxygenation prior to the GOE, such as the Cr isotopes discussed above, have been interpreted as transient "oxygen oases", effectively temporary refugia where O_2 was being produced and aerobic metabolisms could have been established. In this sense, oxygen oases are often viewed as being relatively small or short-lived, akin to a 'whiff' of O_2 (e.g. Anbar et al. 2007). Earth systems models predict that while much of the open ocean in the Archean would have been devoid of O_2, in oxygen oases local O_2 concentrations could have been as high as 1–10 mM (Olson et al. 2013). Nevertheless, how long-lived and extensive such oases were remains to be answered. A recent study on the Pongola and Witwatersrand supergroups by Smith et al. (2023) found carbonate concretions with depleted $\delta^{13}C$ and Mn enrichments, suggesting that free O_2 in the environment was present over a much wider area and for longer than previously thought. The authors suggested that the free O_2 led to the deposition of MnO_2 and subsequent respiration by bacteria yielded the isotopically depleted Mn(II)-rich carbonate concretions. Constraining the extent and longevity of early oxygenation events highlights the need for continuing to study Archean to Paleoproterozoic IF.

IRON FORMATIONS AS PROXIES FOR EARTH'S OXYGENATION

According to the hypothesis presented by Zahnle et al. (2006), the accumulation of O_2 in the atmosphere was hindered by its high chemical reactivity with biogenic CH_4, so as long as CH_4 production remained high, O_2 could not accumulate into the atmosphere. Their model proposed that oxidative weathering of sulphide minerals on land increased the supply of dissolved sulphate to the oceans, leading to the ecological dominance of sulphate-reducing bacteria (SRB) over methanogens around 2.4 Ga as the former can exhaust the supply of labile C_{org} and H_2 that both types of bacteria use as electron donors in their metabolisms. Additionally, the anaerobic (microbial) oxidation of CH_4 by SO_4^{2-} would have suppressed the release of CH_4 from sediments due to increasing SO_4^{2-} concentrations during that period (Catling et al. 2007). However, evidence in the rock record for widespread oxidative weathering of terrestrial sulphide phases, a significant oceanic sulphate reservoir, and the onset of widespread ocean euxinia only appears after the GOE (Poulton et al. 2004; Reinhard et al. 2009). An alternative hypothesis proposed by Konhauser et al. (2009) suggested that the decline in large-scale methanogenesis occurred prior to, and not necessarily because of, increasing environmental oxygenation. Their model indicates a specific progression in Earth's system evolution, where a cooler mantle after 2.7 Ga initiated chemical changes in volcanism and trace element abundances in the oceans, leading to a decline in global methanogenesis. Ultimately, this facilitated the transition from anoxic to oxic atmospheric conditions at approximately 2.45 Ga.

The connection between the decline of methanogens and the rise of cyanobacteria may not be coincidental. In a competitive environment where microorganisms vie for resources, the success of one species can suppress others through competitive exclusion (Hibbing et al. 2010; Weber et al. 2014). A given bacterium can enhance its competitive advantage by producing antimicrobial compounds or evolving resistance to external chemicals. While no pathogenic species have been identified among methanogens, they possess toxin/antitoxin systems (Cavicchioli et al. 2003). Furthermore, a study on acidic peat bogs demonstrated that the addition of the antibiotic rifampicin inhibited the growth of acetogens without affecting the growth of methanogens (Bräuer et al. 2004). It is plausible that pre-2.7 Ga, methanogens were simply more competitive than cyanobacteria and thus widely distributed throughout the oceans, ranging from shallow waters to the sediment. In addition, based on predictions of evolving Fe:P ratios in Precambrian upwelling waters, Jones et al. (2015) suggested that photoferrotrophs would likely have fared better than the cyanobacteria while the oceans were highly ferruginous (with Fe:P > 424, as based on the Redfield ratio). But, as soon as the dissolved Fe:P ratio fell below 424, iron would be exhausted, leaving P to fuel other modes of photoautotrophy, such as oxygenic photosynthesis. Similarly, Swanner et al. (2015) demonstrated experimentally that highly ferruginous waters may have been toxic to cyanobacteria due to the accumulation of reactive oxygen species (ROS) within the cells, resulting in decreased photosynthetic efficiency and slower growth rates. Rampant methanogenesis, whether supported by higher H_2 fluxes or organic matter produced by anoxygenic phototrophy, would have contributed to the maintenance of the largely anoxic conditions. Consequently, this allowed for the dispersal of Fe(II), which would have hindered cyanobacterial proliferation if the Fe(II)-related limitations identified by Jones et al. (2015) and Swanner et al. (2015) were indeed crucial factors. Further, Mloszewska et al. (2018) experimentally demonstrated that unattenuated ultraviolet radiation (uv-C) induces high rates of mortality for planktonic cyanobacteria in the upper reaches of the water column, thus implying that cyanobacterial expansion of the ancient oceans would have been suppressed.

Around 2.7 Ga, a combination of factors coincided that would have promoted a decline in methanogens and the simul-

taneous rise of cyanobacteria, in addition to the decrease in seawater Ni concentrations. The emergence of new continents led to an increased supply of solutes and sediment through weathering processes (Lalonde and Konhauser 2015; Wu et al. 2023), which resulted in the development of stable continental platforms with nutrient-rich, shallow waters favourable for colonization by both benthic and planktonic cyanobacteria (although see Sánchez Baracaldo 2015 for an alternate opinion that planktonic cyanobacteria did not evolve until around 800 Ma). The timing correlates well with the diversification of marine stromatolites (McNamara and Awramik 1992). Indeed, genomic data for extant cyanobacteria have led to the suggestion that multicellularity in cyanobacteria evolved perhaps 200–300 Myr before the GOE (Schirrmeister et al. 2013). The transition to multicellularity represents an important change in organism complexity because filamentous growth can improve cell motility which would allow for movement over sediment, while cooperation of cells can increase metabolic fitness and diversification compared to single cells (e.g. Knoll 1984; Bonner 1998; Koschwanez et al. 2011). Collectively this could have led to new adaptive strategies such as the formation of microbial mats (Sánchez Baracaldo et al. 2022). Moreover, the increased consumption of CO_2 by cyanobacteria led to widespread deposition of calcium carbonate on the seafloor, forming thick beds that extended across vast areas spanning thousands of square kilometres (Grotzinger and Knoll 1999) to facilitate benthic cyanobacterial growth and their calcification throughout the shallow littoral zones. Overall, the combination of stable continental platforms, the evolution of motile and large filamentous cyanobacteria, and increased nutrient supply created an environment where cyanobacteria thrived and produced increasing amounts of O_2, further driving the decline of methanogens.

A decrease in methanogen populations may also have been caused by declining fluxes of H_2 due to diminishing serpentinization of the seafloor. This may have coincided with the reduction in olivine-rich oceanic crust production at the end of the 2.7 Ga mantle plume event and the stabilization of continental cratons (Barley et al. 2005). According to Kump and Barley (2007), the transition from predominantly submarine volcanism to more subaerial volcanism further contributed to the decrease in abiotic H_2 fluxes, as subaerial volcanism releases more oxidized gases such as H_2O, CO_2 and SO_2. Alternatively, Gaillard et al. (2011) proposed that a decrease in volcanic degassing pressure associated with the growth of continental crust led to higher emissions of H_2 which then escaped to space, thus resulting in a net gain of atmospheric O_2. In either case, the diminishing supply of H_2 would have played a role in the decline of biogenic CH_4 production (Kharecha et al. 2005), even if methanogens continued to grow directly on the seafloor crust, where both Ni and H_2 sources remained locally abundant (e.g. Brazelton et al. 2006; Amend et al. 2011).

A third factor which may have contributed to a decline of methanogens and simultaneous proliferation of cyanobacteria was changing seawater Fe^{2+} concentrations. Dissolved iron episodically declined in the shallow regions of continental shelves due to the cessation of plume-driven submarine volcanism and a lowering of sea level. This change created the conditions required for the development of oxygen oases on semi-restricted carbonate platforms, exemplified by extensive stromatolites in the 2.65–2.46 Ga Campbellrand Subgroup in South Africa (Sumner 1997). The existence of dissolved O_2 in seawater along the slope is inferred from various indicators. Shifts towards heavier N isotopes in shale organic carbon indicate the onset of an oxygenated N cycle (Godfrey and Falkowski 2009). Variations in abundances of rhenium (Re) and Mo in shale reflect cycling of these elements in deep oxygenated seawater (Kendall et al. 2010), while the rimmed margins of the platform, as described by Sumner and Beukes (2006), could have provided sheltered lagoons where cyanobacteria thrived, protected from the delivery of Fe(II)-rich water sourced from the deeper regions. This is supported by the deposition of Fe-rich shale along the slope and IF deeper in the basin (Klein and Beukes 1989). The geochemical indicators of O_2 then disappeared during transgressions when deep seawater flooded the platform with Fe(II)-rich waters thought to have been sourced from plume-driven submarine volcanism (Barley et al. 2005).

Evidence for a shift from a CH_4-dominated ocean to an ocean dominated by cyanobacteria is clearly observed in the 150-million-year section (2.72–2.57 Ga) of late Archean shallow- and deep-water sediments found in the Hamersley Basin in Western Australia. In a study by Eigenbrode and Freeman (2006), $\delta^{13}C_{org}$ values were reported for 175 kerogen samples, ranging from –57 to –28‰. The oldest samples contained the most depleted isotopic values, which can be best explained by biological CH_4 assimilation and oxidation by methanotrophic microorganisms. Methane oxidation requires electron acceptors such as O_2, NO_3^-, or SO_4^{2-}. The latter two indirectly depend on O_2 to form oxidized species, although there have been models (e.g. Konhauser et al. 2005) and experimental evidence (Beal et al. 2009) suggesting that Fe(III) can also function as electron acceptor for microorganisms to oxidize CH_4. Therefore, methanotrophy may not necessarily be linked to O_2.

Interestingly, a δ^{13}Corg shift of 29‰ in the kerogens occurred in shallow water carbonate sediment (changing from –57 to –28‰) over that time, while only a 5‰ shift (–45 to –40‰) was observed in the deep water sediment. These patterns indicate a gradual transition in shallow waters from a microbial habitat strongly influenced by CH_4 cycling at 2.72 Ga to one that was more influenced by oxygenic photosynthesis by 2.57 Ga (Eigenbrode and Freeman 2006): cyanobacteria tend to fractionate carbon between –20‰ to –30‰ (e.g. Garcia et al. 2021). In deeper settings, the kerogens remained highly ^{13}C-depleted, indicating that these environments continued to be dominated by communities involved in CH_4 production and consumption and were not yet affected by the significant changes in carbon cycling occurring in shallow waters. By comparing the data from the Hamersley Basin to other locations, Eigenbrode and Freeman (2006) further suggested that a global-scale expansion of oxygenated habitats coincided with the transition from anoxic ecosystems to microbial communities fueled by oxygenic photosynthesis, occurring before the oxygenation of the atmosphere 2.45 Ga.

Around 2.45 Ga, as the GOE began, aerobic chemolithoautotrophic weathering of pyrite on land caused a significant increase in acidity which led to an elevated flux of solutes, which were previously low due to their insolubility under an anoxic atmosphere at the Earth's crustal surface (Konhauser et al. 2011). One specific example relevant to the earlier discussion is SO_4^{2-}, which started to appear in significant concentrations in the marine environment around 2.5 Ga (Reinhard et al. 2009). The accumulation of SO_4^{2-} in the oceans continued until around 2.0 Ga (Planavsky et al. 2012b; Blättler et al. 2018), when it is believed that atmospheric O_2 levels started to decline (Partin et al. 2013; Scott et al. 2014), marking the beginning of what is commonly referred to as Earth's "boring billion" period. With the increased supply of SO_4^{2-} to the oceans, marine SRB would have begun to dominate the anoxic regions of the water column. This further marginalized the methanogens, relegating them to sulphate-poor sediment, like their current distribution. As a consequence of the progressive decline in methane production, which is a potent greenhouse gas, the climate started to cool, eventually leading to significant Paleoproterozoic glaciations (Zahnle et al. 2006).

Concomitant with increased acidity was also the supply of other insoluble elements to seawater. Konhauser et al. (2011) argued that the increased concentrations of Cr in IF between 2.45 to 2.32 Ga was due to the mobilization of Cr(III) from both ultramafic rocks and soils. Specifically, those authors suggested that dissolved Cr^{3+} or $Cr(OH)^{2+}$ was then transported to the oceans via acidic streams or groundwater, and upon mixing with seawater, would have rapidly precipitated out of solution as a $(Fe,Cr)(OH)_3$ phase that became incorporated in IF. However, streams and groundwater with low pH would be naturally buffered by more alkaline waters flowing through non-acid-generating rock types (i.e. silicate-weathering reactions that control the inorganic carbon system). Therefore, much of the Cr(III) mobilized by this pulse of low-pH oxidative weathering presumably never made it to the oceans, instead being lost from solution along catchment pathways. To address this apparent contradiction, Hao et al. (2022) sought an alternative mode of Cr transport, namely the erosion and subsequent transport of suspended sediment with anomalous Cr enrichments. In an experimental study designed to test the complexation of Cr(III) to common soil clay minerals, the authors demonstrated that Cr(III) was strongly bound to kaolinite in particular under acidic conditions and weakly desorbed under marine conditions. Extending those results to the interpretation of the Cr record in IF, Hao et al. (2022) suggested that under intense chemical weathering conditions, not only did acidity promote the solubilization of Cr(III) from primary Cr(III)-bearing minerals, but that parent rocks were more systematically weathered to an advanced state dominated by kaolinite – creating ideal conditions for Cr adsorption. Erosion of regolith that scavenged mobilized Cr(III) could then facilitate transport of Cr(III)-bearing kaolinite – the "kaolinite shuttle" – to coastal environments where it contributed to the high Cr abundances preserved in the Paleoproterozoic IF.

Konhauser et al. (2011) also concluded that acidity would have solubilized minerals that contained nutrients, e.g. apatite, releasing dissolved P, and thus leading to increased nutrient supply to the oceans and enhanced primary productivity. Bekker and Holland (2012) further argued that the largest positive carbon isotope excursion, the so-called the Lomagundi Event (LE), ca. 2.22 to 2.06 Ga, was caused by such an acidic P flux from land. It has been widely argued – though not universally agreed upon – that the LE marks a period of enhanced organic C_{org} burial (e.g. cyanobacteria), such that the isotopically light carbon was incorporated into the sediment pile while the isotopically heavy carbon was incorporated into marine carbonate minerals (see Schidlowski et al. 1976 but see also Mayika et al. 2020 and Prave et al. 2022 for alternative views). By this model, the extensive burial of cyanobacterial biomass led to the accumulation of O_2 in the atmosphere. In fact, it has been hypothesized that during the LE, Earth's surface environments experienced a release of O_2 to the extent of 12 to 22 times the present atmospheric O_2 inventory (Karhu and Holland 1996).

Nonetheless, the question remains: how did the dissolved phosphorus released during acid weathering find its way from land to the oceans? In the present day, most of the P delivered to the oceans is in the form of suspended sediment, with less than 10% of total P being transported as dissolved anions through rivers (Berner and Rao 1994). Similar to the Cr story, P is predominantly transported as a particulate phase, including P adsorbed onto iron(III)-aluminum(III)-oxyhydroxides or clay minerals, or complexed with organic matter (Gérard 2016). A significant portion of adsorbed P settles in estuaries and marginal marine environments through the flocculation of particulate phases, where it remains inaccessible to plankton until remobilization within the sediment pile (Conley et al. 1995). In the absence of plants, the only organic compounds transported to the oceans would have originated from degraded continental microbial mats (e.g. Lalonde and Konhauser 2015), which are unlikely to have had a significant impact on the P cycle. Moreover, during the LE, iron oxyhydroxides would have been solubilized in sulphide-rich soils, like observations in certain black shale weathering environments today (e.g. Joeckel et al. 2005). Expanding on this framework, Hao et al. (2021) demonstrated that the main mechanism by which P was delivered to the oceans during that time was likely through an active kaolinite shuttle. However, unlike Cr, P quickly desorbs from kaolinite when exposed to marine conditions. Importantly, the authors also conducted experiments showing that the released P was bioavailable to marine cyanobacteria. In one culture lacking P input, the cyanobacteria entered a death phase by day 14, while the culture 'seeded' with P-bearing kaolinite resulted in a population of cells that exponentially increased in density. In summary, the high adsorption capacity of kaolinite for P under acidic, freshwater conditions, coupled with its low capacity under alkaline, marine conditions, enhanced P bioavailability and promoted cyanobacterial productivity in nearshore environments after the GOE.

https://doi.org/10.12789/geocanj.2023.50.201

On a final note, it is worth noting that during the GOE, certain oxidized compounds were mobilized for the first time, posing a toxic threat to microbes that had evolved in O_2-deprived marine environments. One example is arsenate, the pentavalent oxidized form of arsenic (As), which exhibits toxicity to all three domains of life even at very low concentrations and shows a strong inverse correlation with marine primary production (e.g. Smedley and Kinniburgh 2002). It has been proposed that the widespread deposition of IF during the transition from the Archean to the Paleoproterozoic facilitated the preferential incorporation of P over As(V) into ferric oxyhydroxides like ferrihydrite. This resulted in a simultaneous increase in As(V) concentration and depletion of P in seawater, negatively impacting marine primary productivity (Chi Fru et al. 2016; Hemmingsson et al. 2018). A study conducted by Chi Fru et al. (2019), which analyzed sedimentary rocks spanning from 2.9 to 1.9 Ga, further demonstrated that the GOE coincided with a significant rise in arsenate levels in IF and the presence of arsenic sulphides in marine shale. This notable increase in O_2-sensitive tracers aligns with the proliferation of key arsenic oxidants, including O_2, NO_3^-, and MnO_2. The substantial surge in arsenic sulphides by at least tenfold after 2.45 billion years ago supports the hypothesis of a transition to sulphide-rich waters at mid-depth continental margins following the GOE. Additionally, the substantial elevation in arsenate content, accounting for approximately 60% of the total arsenic concentration in shale, suggests the establishment of an oxidative component in the arsenic cycle for the first time in Earth's history. These findings underscore the worldwide emergence of a new selective pressure on the survival of marine microbial communities during the GOE, characterized by the global presence of toxic, oxidized species such as arsenate in seawater.

CONCLUSION

In this contribution we aimed to integrate available geochemical data from IF into a coherent narrative explaining the mechanisms underpinning the rise of atmospheric O_2 and its subsequent regulation of Earth's surface systems. The sequence begins with a cooling Earth around 2.7 Ga, leading to the eruption of lavas with lower Ni content both on land and underwater. As these volcanic rocks contained less Ni, their chemical weathering resulted in a reduced flux of Ni to seawater. This had biological implications as marine microorganisms dependent on Ni, such as methanogens, started experiencing nutrient deprivation. Around 2.6 Ga, methanogens became marginalized in shallow shelf environments, making way for cyanobacterial expansion, which gave rise to new stromatolites. Before the GOE and the permanent oxygenation of Earth's atmosphere, the O_2 produced by these cyanobacteria created oxygen oases that facilitated the development of aerobic metabolisms. Constraining the extent of such oases with respect to both space and time presents an opportunity to continue to integrate detailed geochemical and sedimentological observations from IFs and correlative units.

By approximately 2.45 Ga, O_2 had becoming increasingly pervasive in Earth surface environments, oxygenating the atmosphere and marking the GOE. This event resulted in massive oxidative weathering of the Earth's crust and the release of elements previously locked in reduced mineral phases, such as pyrite. Concurrently, aerobic metabolisms evolved on land, including chemolithoautotrophic bacteria that oxidized reduced Fe and S in minerals such as pyrite. Increased fluxes of dissolved SO_4^{2-} reached the oceans, leading to greater bacterial sulphate reduction in the water column. This resulted in higher levels of dissolved sulphide, the production of euxinic waters (low oxygen, sulphidic conditions), and the terminal displacement of methanogens from the water column to bottom sediments in most environments. Pyrite oxidation also led to elevated acidity in rivers and groundwater, promoting the chemical alteration of primary minerals into highly weathered phases like kaolinite (Fig. 7). Importantly, kaolinite served as an elemental shuttle, facilitating the increased availability of key nutrients such as P, which, in turn, stimulated higher primary productivity. Intriguingly, the ability of cyanobacteria to indirectly enhance their own nutrient supply through O_2-driven chemical weathering may represent an unrecognized positive biological feedback mechanism on primary productivity. This scenario is reminiscent of the Gaia hypothesis where the Earth functions as a self-regulating system with the geosphere, atmosphere, hydrosphere, and biosphere all interconnected and evolving as a whole (Lovelock 1972). The Lomagundi carbon isotope excursion around 2.22 Ga may be an expression of these feedbacks, ultimately resulting in increased marine phytoplankton productivity and organic matter burial. Simultaneously, toxic elements like As would have affected the existing

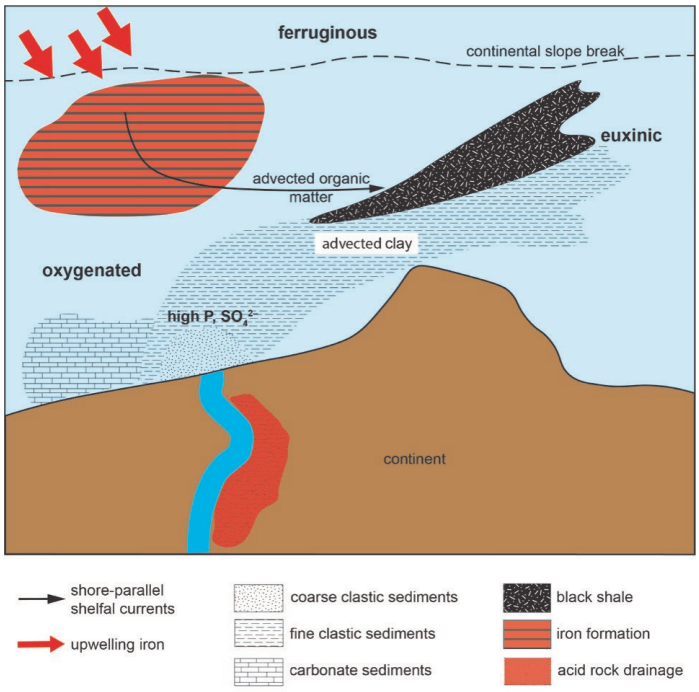

Figure 7. Schematic showing the spatial distribution of iron formations (IF), siliciclastic and carbonate sediments on the Archean continental shelf. The panel also emphasizes how plankton could be advected from the shelf where IF were precipitated to become incorporated into black shale. Prevailing redox conditions and nutrient supplies are indicated in bold text.

marine biosphere, prompting some species to adapt while potentially leading to the extinction of others. In this regard, it is intriguing to speculate that the end of the Lomagundi event, which appears to have coincided with a significant drop in atmospheric O_2 levels, may be somehow linked to a microbial mass extinction, or at the very least, marginalization of those existing cyanobacteria due to some unresolved factor.

ACKNOWLEDGEMENTS

The lead author extends gratitude to the Geological Association of Canada for the honour of receiving the Logan Medal. The content presented in this work represents a concise overview of more than twenty years of research, a feat made possible through the dedicated contributions of numerous graduate students who gathered samples from various corners of the globe, conducted a wide array of geochemical and mineralogical analyses, amalgamated their findings, and, in the end, published our collective data. Additionally, I wish to express appreciation for the financial assistance provided by the Natural Sciences and Engineering Research Council of Canada.

REFERENCES

Albut, G., Babechuk, M.G., Kleinhanns, I.C., Benger, M., Beukes, N.J., Steinhilber, B., Smith, A.J.B., Kruger, S.J., and Schoenberg, R., 2018, Modern rather than Mesoarchaean oxidative weathering responsible for the heavy stable Cr isotopic signatures of the 2.95 Ga old Ijzermijn iron formation (South Africa): Geochimica et Cosmochimica Acta, v. 228, p. 157–189, https://doi.org/10.1016/j.gca.2018.02.034.

Albut, G., Kamber, B.S., Brüske, A., Beukes, N.J., Smith, A.J.B, and Schoenberg, R., 2019, Modern weathering in outcrop samples versus ancient paleoredox information in drill core samples from a Mesoarchaean marine oxygen oasis in Pongola Supergroup, South Africa: Geochimica et Cosmochimica Acta, v. 265, p. 330–353, https://doi.org/10.1016/j.gca.2019.09.001.

Alexander, B.W., Bau, M., Andersson, P., and Dulski, P., 2008, Continentally-derived solutes in shallow Archean seawater: Rare earth element and Nd isotope evidence in iron formation from the 2.9 Ga Pongola Supergroup, South Africa: Geochimica et Cosmochimica Acta, v. 72, p. 378–394, https://doi.org/10.1016/j.gca.2007.10.028.

Amend, J.P., McCollom, T.M., Hentscher, M., and Bach, W., 2011, Catabolic and anabolic energy for chemolithoautotrophs in deep-sea hydrothermal systems hosted in different rock types: Geochimica et Cosmochimica Acta, v. 75, p. 5736–5748, https://doi.org/10.1016/j.gca.2011.07.041.

Anbar, A.D., and Knoll, A.H., 2002, Proterozoic ocean chemistry and evolution: a bioinorganic bridge?: Science, v. 297, p. 1137–1142, https://doi.org/10.1016/j.gca.2011.07.041.

Anbar, A.D., Duan, Y., Lyons, T.W., Arnold, G.L., Kendall, B., Creaser, R.A., Kaufman, A.J., Gordon, G.W., Scott, C., Garvin, J., and Buick, R., 2007, A whiff of oxygen before the Great Oxidation Event?: Science, v. 317, p. 1903–1906, https://doi.org/10.1126/science.1140325.

Barley, M.E., Bekker, A., and Krapež, B., 2005, Late Archean to early Paleoproterozoic global tectonics, environmental change and the rise of atmospheric oxygen: Earth and Planetary Science Letters, v. 238, p. 156–171, https://doi.org/10.1016/j.epsl.2005.06.062.

Bau, M., and Dulski, P., 1996, Distribution of yttrium and rare-earth elements in the Penge and Kuruman iron-formations, Transvaal Supergroup, South Africa: Precambrian Research v. 79, p. 37–55, https://doi.org/10.1016/0301-9268(95)00087-9.

Bau, M., and Möller, P., 1993, Rare earth element systematics of the chemically precipitated component in early Precambrian iron formations and the evolution of the terrestrial atmosphere-hydrosphere-lithosphere system: Geochimica et Cosmochimica Acta: v. 57, p. 2239–2249, https://doi.org/10.1016/0016-7037(93)90566-F.

Baur, M.E., Hayes, J.M., Studley, S.A., and Walter, M.A., 1985, Millimeter-scale variations of stable isotope abundances in carbonates from banded iron-formations in the Hamersley Group of Western Australia: Economic Geology, v. 80, p. 270–282, https://doi.org/10.2113/gsecongeo.80.2.270.

Beal, E.J., House, C.H., and Orphan, V.J., 2009, Manganese- and iron-dependent marine methane oxidation: Science, v. 325, p. 184–187, https://doi.org/10.1126/science.1169984.

Bekker, A., and Holland, H.D., 2012, Oxygen overshoot and recovery during the early Paleoproterozoic: Earth and Planetary Science Letters, v. 317–318, p. 295–304, https://doi.org/10.1016/j.epsl.2011.12.012.

Bekker, A., Slack, J.F., Planavsky, N., Krapež, B., Hofmann, A., Konhauser, K.O., and Rouxel, O.J., 2010, Iron formation: The sedimentary product of a complex interplay among mantle, tectonic, oceanic, and biospheric processes: Economic Geology, v. 105, p. 467–508, https://doi.org/10.2113/gsecongeo.105.3.467.

Berner, R.A., and Rao, J.-L., 1994, Phosphorus in sediments of the Amazon River and estuary - Implications for the global flux of phosphorus to the sea: Geochimica et Cosmochimica Acta, v. 58, p. 2333–2339, https://doi.org/10.1016/0016-7037(94)90014-0.

Beukes, N.J., and Gutzmer, J., 2008, Origin and paleoenvironmental significance of major iron formations at the Archean-Paleoproterozoic boundary, *in* Hagemann, S., Rosière, C.A., Gutzmer, J., and Beukes, N.J., *eds.,* Banded Iron Formation-Related High-Grade Iron Ore: Reviews in Economic Geology, v. 15, p. 5–47, https://doi.org/10.5382/Rev.15.01.

Bjerrum, C.J., and Canfield, D.E., 2002, Ocean productivity before about 1.9 Gyr ago limited by phosphorus adsorption onto iron oxides: Nature, v. 417, p. 159–162, https://doi.org/10.1038/417159a.

Blättler, C.L., Claire, M.W., Prave, A.R., Kirsimäe, K., Higgins, J.A., Medvedev, P.V., Romashkin, A.E., Rychanchik, D.V., Zerkle, A.L., Paiste, K., Kreitsmann, T., Millar, I.L., Hayles, J.A., Bao, H., Turchyn, A.V., Warke, M.R., and Lepland, A., 2018, Two-billion-year-old evaporites capture Earth's great oxidation: Science, v. 360, p. 320–323, https://doi.org/10.1126/science.aar2687.

Boden, J.S., Konhauser, K.O., Robbins, L.J., and Sánchez-Baracaldo, P., 2021, Timing the evolution of antioxidant enzymes in cyanobacteria: Nature Communications, v. 12, 4742, https://doi.org/10.1038/s41467-021-24396-y.

Bolhar, R., Kamber, B.S., Moorbath, S., Fedo, C.M., and Whitehouse, M.J., 2004, Characterization of early Archaean chemical sediments by trace element signatures: Earth and Planetary Science Letters, v. 222, p. 43–60, https://doi.org/10.1016/j.epsl.2004.02.016.

Bonner, J.T., 1998, The origins of multicellularity: Integrative Biology, v. 1, p. 27–36, https://doi.org/10.1002/(SICI)1520-6602(1998)1:1<27::AID-INBI4>3.0.CO;2-6.

Brady, M.P., Tostevin, R., and Tosca, N.J., 2022, Marine phosphate availability and the chemical origins of life on Earth: Nature Communications, v. 13, 5162, https://doi.org/10.1038/s41467-022-32815-x.

Bräuer, S.L., Yavitt, J.B., and Zinder, S.H., 2004, Methanogenesis in McLean Bog, an acidic peat bog in upstate New York: stimulation by H_2/CO_2 in the presence of rifampicin, or by low concentrations of acetate: Geomicrobiology Journal, v. 21, p. 433–443, https://doi.org/10.1080/01490450490505400.

Brazelton, W.J., Schrenk, M.O., Kelley, D.S., and Baross, J.A., 2006, Methane- and sulfur-metabolizing microbial communities dominate the Lost City Hydrothermal Field ecosystem: Applied and Environmental Microbiology, v. 72, p. 6257–6270, https://doi.org/10.1128/AEM.00574-06.

Bruland, K.W., Middag, R., and Lohan, M.C., 2014, Controls of trace metals in seawater, *in* Holland, H.D., and Turekian, K.K., *eds.,* Treatise on Geochemistry (Second Edition). Elsevier, Oxford, p. 19–51, https://doi.org/10.1016/B978-0-08-095975-7.00602-1.

Canfield, D.E., 1998, A new model for Proterozoic ocean chemistry: Nature, v. 396, p. 450–453, https://doi.org/10.1038/24839.

Catling, D.C., Claire, M.W., and Zahnle, K.J., 2007, Anaerobic methanotrophy and the rise of atmospheric oxygen: Philosophical Transactions of the Royal Society A, v. 365, p. 1867–1888, https://doi.org/10.1098/rsta.2007.2047.

Cavicchioli, R., Curmi, P.M.G., Saunders, N., and Thomas, T., 2003, Pathogenic archaea: do they exist?: BioEssays, v. 25, p. 1119–1128, https://doi.org/10.1002/bies.10354.

Chan, C.S., Emerson, D., and Luther, G.W., 2016, The role of microaerophilic Fe-oxidizing micro-organisms in producing banded iron formations: Geobiology, v. 14, p. 509–528, https://doi.org/10.1111/gbi.12192.

Chi Fru, E., Rodríguez, N.P., Partin, C.A., Lalonde, S.V., Andersson, P.S., Weiss, D.J., El Albani, A., Rodushkin, I., and Konhauser, K.O., 2016, Cu isotopes in marine black shales record the Great Oxidation Event: Proceedings of the National Academy of Sciences, v. 113, p. 4941–4946, https://doi.org/10.1073/pnas.1523544113.

Chi Fru, E., Somogyi, A., El Albani, A., Medjoubi, K., Aubineau, J., Robbins, L.J., Lalonde, S.V., and Konhauser, K.O., 2019, The rise of oxygen-driven arsenic cycling at ca. 2.48 Ga: Geology, v. 47, p. 243–246, https://doi.org/10.1130/G45676.1.

Cloud, P.E., Jr., 1965, Significance of the Gunflint (Precambrian) microflora: Science, v. 148, p. 27–35, https://doi.org/10.1126/science.148.3666.27.

Condie, K.C., 1993, Chemical composition and evolution of the upper continental crust: contrasting results from surface samples and shales: Chemical Geology, v. 104, p. 1–37, https://doi.org/10.1016/0009-2541(93)90140-E.

Conley, D.J., Smith, W.M., Cornwell, J.C., and Fisher, T.R., 1995, Transformation of particle-bound phosphorus at the land-sea interface: Estuarian, Coastal and

Shelf Science, v. 40, p. 161–176, https://doi.org/10.1016/S0272-7714(05)80003-4.
Craddock, P.R., and Dauphas, N., 2011, Iron and carbon isotope evidence for microbial iron respiration throughout the Archean: Earth and Planetary Science Letters, v. 303, p. 121–132, https://doi.org/10.1016/j.epsl.2010.12.045.
Crowe, S.A., Jones, C., Katsev, S., Magen, C., O'Neill, A.H., Sturm, A., Canfield, D.E., Haffner, G.D., Mucci, A., Sundby, B., and Fowle, D.A., 2008, Photoferrotrophs thrive in an Archean ocean analogue: Proceedings of the National Academy of Sciences, v. 105, p. 15938–15943, https://doi.org/10.1073/pnas.0805313105.
Crowe, S.A. Katsev, S., Leslie, K., Sturm, A., Magen, C., Nomosatryo, S., Pack, M.A., Kessler, J.D., Reeburgh, W.S., Roberts, J.A., González, L., Haffner, G.D., Mucci, A., Sundby, B., and Fowle, D.A., 2011, The methane cycle in ferruginous Lake Matano: Geobiology, v. 9, p. 61–78, https://doi.org/10.1111/j.1472-4669.2010.00257.x.
Crowe, S.A., Døssing, L.N., Beukes, N.J., Bau, M., Kruger, S.J., Frei, R., and Canfield, D.E., 2013, Atmospheric oxygenation three billion years ago: Nature, v. 501, p. 535–538, https://doi.org/10.1038/nature12426.
Czaja, A.D., Johnson, C.M., Beard, B.L., Roden, E.E., Li, W., and Moorbath, S., 2013, Biological Fe oxidation controlled deposition of banded iron formation in the ca. 3370 Ma Isua Supracrustal Belt (West Greenland): Earth and Planetary Science Letters, v. 363, p. 192–203, https://doi.org/10.1016/j.epsl.2012.12.025.
Derry, L.A., 2015, Causes and consequences of mid Proterozoic anoxia: Geophysical Research Letters, v. 42, p. 8538–8546, https://doi.org/10.1002/2015GL065333.
Dorland, H.C., 1999, Paleoproterozoic Laterites, Red Beds and Ironstones of the Pretoria Group With Reference to the History of Atmospheric Oxygen: Unpublished MSc Thesis, Rand Afrikaans University, Johannesburg, South Africa, 147 p.
Døssing, L.N., Dideriksen, K., Stipp, S.L.S., and Frei, R., 2011, Reduction of hexavalent chromium by ferrous iron: A process of chromium isotope fractionation and its relevance to natural environments: Chemical Geology, v. 285, p. 157–166, https://doi.org/10.1016/j.chemgeo.2011.04.005.
Eickhoff, M., Obst, M., Schröder, C., Hitchcock, A.P., Tyliszczak, T., Martinez, R.E., Robbins, L.J., Konhauser, K.O., and Kappler, A., 2014, Nickel partitioning in biogenic and abiogenic ferrihydrite: The influence of silica and implications for ancient environments: Geochimica et Cosmochimica Acta, v. 140, p. 65–79, https://doi.org/10.1016/j.gca.2014.05.021.
Eigenbrode, J.L., and Freeman, K.H., 2006, Late Archean rise of aerobic microbial ecosystems: Proceedings of the National Academy of Sciences, v. 103, p. 15759–15764, https://doi.org/10.1073/pnas.0607540103.
Ellis, A.S., Johnson, T.M., and Bullen, T.D., 2002, Chromium isotopes and the fate of hexavalent chromium in the environment: Science, v. 295, p. 2060–2062, https://doi.org/10.1126/science.1068368.
Feely, R.A., Trefry, J.H., Lebon, G.T., and German, C.R., 1998, The relationship between P/Fe and V/Fe ratios in hydrothermal precipitates and dissolved phosphate in seawater: Geophysical Research Letters, v. 25, p. 2253–2256, https://doi.org/10.1029/98GL01546.
Fischer, W.W., and Knoll, A.H., 2009, An iron shuttle for deepwater silica in Late Archean and early Paleoproterozoic iron formation: Geological Society of America Bulletin, v. 121, p. 222–235, https://doi.org/10.1130/B26328.1.
Frausto da Silva, J.J.R., and Williams, R.J., 2001, The Biological Chemistry of the Elements: The Inorganic Chemistry of Life (2nd ed.): Oxford University Press, Oxford, UK, 600 p.
Frei, R., Gaucher, C., Poulton, S.W., and Canfield, D.E., 2009, Fluctuations in Precambrian atmospheric oxygenation recorded by chromium isotopes: Nature, v. 461, p. 250–253, https://doi.org/10.1038/nature08266.
Frost, C.D., von Blanckenburg, F., Schoenberg, R., Frost, B.R., and Swapp, S.M., 2007, Preservation of Fe isotope heterogeneities during diagenesis and metamorphism of banded iron formation: Contributions to Mineralogy and Petrology, v. 153, p. 211–235, https://doi.org/10.1007/s00410-006-0141-0.
Gaillard, F., Scaillet, B., and Arndt, N.T., 2011, Atmospheric oxygenation caused by a change in volcanic degassing pressure: Nature, v. 478, p. 229–232, https://doi.org/10.1038/nature10460.
Garcia, A.K., Cavanaugh, C.M., and Kacar, B., 2021, The curious consistency of carbon biosignatures over billions of years of Earth-life coevolution: The ISME Journal, v. 15, p. 2183–2194, https://doi.org/10.1038/s41396-021-00971-5.
Gauger, T., Byrne, J.M., Konhauser, K.O., Obst, M., Crowe, S., and Kappler, A., 2016, Influence of organics and silica on Fe(II) oxidation rates and cell–mineral aggregate formation by the green-sulfur Fe(II)-oxidizing bacterium *Chlorobium ferrooxidans* KoFox – Implications for Fe(II) oxidation in ancient oceans: Earth and Planetary Science Letters, v. 443, p. 81–89, https://doi.org/10.1016/j.epsl.2016.03.022.
Gérard, F., 2016, Clay minerals, iron/aluminum oxides, and their contribution to phosphate sorption in soils – A myth revisited: Geoderma, v. 262, p. 213–226, https://doi.org/10.1016/j.geoderma.2015.08.036.
Godfrey, L.V., and Falkowski, P.G., 2009, The cycling and redox state of nitrogen in the Archaean ocean: Nature Geoscience, v. 2, p. 725–729, https://doi.org/10.1038/ngeo633.
Gole, M.J., and Klein, C., 1981, Banded iron-formations through much of Precambrian time: The Journal of Geology, v. 89, p. 169–183, https://doi.org/10.1086/628578.
Gross, G.A., 1980, A classification of iron-formation based on depositional environments: Canadian Mineralogist, v. 18, p. 215–222.
Grotzinger, J.P., and Knoll, A.H., 1999, Stromatolites in Precambrian carbonates: evolutionary mileposts or environmental dipsticks?: Annual Reviews of Earth and Planetary Sciences, v. 27, p. 313–358, https://doi.org/10.1146/annurev.earth.27.1.313.
Hagemann, S.G., Angerer, T., Duuring, P., Rosière, C.A., Figueiredo e Silva, R.C., Lobato, L., Hensler, A.S., and Walde, D.H.G., 2016, BIF-hosted iron mineral system: A review: Ore Geology Reviews, v. 76, p. 317–359, https://doi.org/10.1016/j.oregeorev.2015.11.004.
Halama, M., Swanner, E.D., Konhauser, K.O., and Kappler, A., 2016, Evaluation of siderite and magnetite formation in BIFs by pressure-temperature experiments of Fe(III) minerals and microbial biomass: Earth and Planetary Science Letters, v. 450, p. 243–253, https://doi.org/10.1016/j.epsl.2016.06.032.
Halevy, I., Alesker, M., Schuster, E.M., Popovitz-Biro, R., and Feldman, Y., 2017, A key role for green rust in the Precambrian oceans and the genesis of iron formations: Nature Geoscience, v. 10, p. 135–139, https://doi.org/10.1038/ngeo2878.
Hao, J., Knoll, A.H., Huang, F., Hazen, R.M., and Daniel, I., 2020, Cycling phosphorus on the Archean Earth: Part I. Continental weathering and riverine transport of phosphorus: Geochimica et Cosmochimica Acta, v. 273, p. 70–84, https://doi.org/10.1016/j.gca.2020.01.027.
Hao, W., Mänd, K., Li, Y., Alessi, D.S., Somelar, P., Moussavou, M., Romashkin, A.E., Lepland, A., Kirsimäe, K., Planavsky, N.J., and Konhauser, K.O., 2021, The kaolinite shuttle links the Great Oxidation and Lomagundi events: Nature Communications, v. 12, 2944, https://doi.org/10.1038/s41467-021-23304-8.
Hao, W., Chen, N., Sun, W., Mänd, K., Kirsimäe, K., Teitler, Y., Somelar, P., Robbins, L.J., Babechuk, M.G., Planavsky, N.J., Alessi, D.S., and Konhauser, K.O., 2022, Binding and transport of Cr(III) by clay minerals during the Great Oxidation Event: Earth and Planetary Science Letters, v. 584, 117503, https://doi.org/10.1016/j.epsl.2022.117503.
Hartman, H., 1984, The evolution of photosynthesis and microbial mats: A speculation on the banded iron formations, *in* Cohen, Y., Castenholz, R.W., and Halvorson, H.O., *eds.,* Microbial Mats: Stromatolites: Alan R. Liss, Incorporated, New York, p. 449–453.
Haugaard, R., Frei, R., Stendal, H., and Konhauser, K.O., 2013, Petrology and geochemistry of the ~2.9 Ga Itilliarsuk banded iron formation and associated supracrustal rocks, West Greenland: Source characteristics and depositional environment: Precambrian Research, v. 229, p. 150–176, https://doi.org/10.1016/j.precamres.2012.04.013.
Hausinger, R.P., 1987, Nickel utilization by microorganisms: Microbiological Reviews, v. 51, p. 22–42, https://doi.org/10.1128/mr.51.1.22-42.1987.
Heimann, A., Johnson, C.M., Beard, B.L., Valley, J.W., Roden, E.E., Spicuzza, M.J., and Beukes, N.J., 2010, Fe, C, and O isotope compositions of banded iron formation carbonates demonstrate a major role for dissimilatory iron reduction in ~ 2.5 Ga marine environments: Earth and Planetary Science Letters, v. 294, p. 8–18, https://doi.org/10.1016/j.epsl.2010.02.015.
Hemmingsson, C., Pitcain, I.K., and Chi Fru, E., 2018, Evaluation of phosphate-uptake mechanisms by Fe(III)(oxyhydr)oxides in early Proterozoic oceanic conditions: Environmental Chemistry, v. 15, p. 18–28, https://doi.org/10.1071/EN17124.
Hibbing, M.E., Fuqua, C., Parsek, M.R., and Peterson, S.B., 2010, Bacterial competition: surviving and thriving in the microbial jungle: Nature Reviews Microbiology, v. 8, p. 15–25, https://doi.org/10.1038/nrmicro2259.
Hoffman, P.F., Kaufman, A.J., Halverson, G.P., and Schrag, D.P., 1998, A Neoproterozoic snowball Earth: Science, v. 281, p. 1342–1346, https://doi.org/10.1126/science.281.5381.1342.
Holland, H.D., 1973, The oceans; A possible source of iron in iron-formations: Economic Geology, v. 68, p. 1169–1172, https://doi.org/10.2113/gsecongeo.68.7.1169.
Holland, H.D., 1978, The Chemistry of the Atmosphere and Oceans: Wiley, New York, 369 p.
Holland, H.D., 1984, The Chemical Evolution of the Atmosphere and Oceans: Princeton University Press, Princeton, NJ, 598 p., https://doi.org/10.1515/

9780691220239.
Homann, M., Sansjofre, P., Van Zuilen, M., Heubeck, C., Gong, J., Killingsworth, B., Foster, I.S., Airo, A., Van Kranendonk, M.J., Ader, M., and Lalonde, S.V., 2018, Microbial life and biogeochemical cycling on land 3,220 million years ago: Nature Geoscience, v. 11, p. 665–671, https://doi.org/10.1038/s41561-018-0190-9.
Immenhauser, A., 2009, Estimating palaeo-water depth from the physical rock record: Earth-Science Reviews, v. 96, p. 107–139, https://doi.org/10.1016/j.earscirev.2009.06.003.
Isley, A.E., 1995, Hydrothermal plumes and the delivery of iron to banded iron formation: The Journal of Geology, v. 103, p. 169–185, https://doi.org/10.1086/629734.
Isley, A.E., and Abbott, D.H., 1999, Plume-related mafic volcanism and the deposition of banded iron formation: Journal of Geophysical Research, v. 104, p. 15461–15477, https://doi.org/10.1029/1999JB900066.
Jabłońska, J., and Tawfik, D.S., 2021, The evolution of oxygen-utilizing enzymes suggests early biosphere oxygenation: Nature Ecology & Evolution, v. 5, p. 442–448, https://doi.org/10.1038/s41559-020-01386-9.
Jiang, C.Z., and Tosca, N.J., 2019, Fe(II)-carbonate precipitation kinetics and the chemistry of anoxic ferruginous seawater: Earth and Planetary Science Letters, v. 506, p. 231–242, https://doi.org/10.1016/j.epsl.2018.11.010.
Joeckel, R.M., Ang Clement, B.J., and VanFleet Bates, L.R., 2005, Sulfate-mineral crusts from pyrite weathering and acid rock drainage in the Dakota Formation and Graneros Shale, Jefferson County, Nebraska: Chemical Geology, v. 215, p. 433–452, https://doi.org/10.1016/j.chemgeo.2004.06.044.
Johnson, C.M., Beard, B.L., Klein, C., Beukes, N.J., and Roden, E.E., 2008, Iron isotopes constrain biologic and abiologic processes in banded iron formation genesis: Geochimica et Cosmochimica Acta, v. 72, p. 151–169, https://doi.org/10.1016/j.gca.2007.10.013.
Johnson, J.E., Muhling, J.R., Cosmidis, J., Rasmussen, B., and Templeton, A.S., 2018, Low Fe (III) greenalite was a primary mineral from Neoarchean oceans: Geophysical Research Letters, v. 45, p. 3182–3192, https://doi.org/10.1002/2017GL076311.
Jones, C., Nomosatryo, S., Crowe, S.A., Bjerrum, C.J., and Canfield, D.E., 2015, Iron oxides, divalent cations, silica, and the early earth phosphorus crisis: Geology, v. 43, p. 135–138, https://doi.org/10.1130/G36044.1.
Kappler, A., Pasquero, C., Konhauser, K.O., and Newman, D.K., 2005, Deposition of banded iron formations by anoxygenic phototrophic Fe(II)-oxidizing bacteria: Geology, v. 33, p. 865–868, https://doi.org/10.1130/G21658.1.
Karhu, J.A., and Holland, H.D., 1996, Carbon isotopes and the rise of atmospheric oxygen: Geology, v. 24, p. 867–870, https://doi.org/10.1130/0091-7613(1996)024<0867:CIATRO>2.3.CO;2.
Kasting, J.F., 2013, What caused the rise of atmospheric O_2?: Chemical Geology, v. 362, p. 13–25, https://doi.org/10.1016/j.chemgeo.2013.05.039.
Kendall, B., Reinhard, C.T., Lyons, T.W., Kaufman, A.J., Poulton, S.W., and Anbar, A.D., 2010, Pervasive oxygenation along late Archaean ocean margins: Nature Geoscience, v. 3, p. 647–652, https://doi.org/10.1038/ngeo942.
Kharecha, P.A., Kasting, J.F., and Siefert, J.L., 2005, A coupled atmosphere-ecosystem model of the early Archean Earth: Geobiology, v. 3, p. 53–76, https://doi.org/10.1111/j.1472-4669.2005.00049.x.
Kipp, M.A., and Stueken, E.E., 2017, Biomass recycling and Earth's early phosphorus cycle: Science Advances, v. 3, eaao4795, https://doi.org/10.1126/sciadv.aao4795.
Klein, C., 2005, Presidential Address to the Mineralogical Society of America, Boston, November 6, 2001: Some Precambrian banded iron-formations (BIFs) from around the world: Their age, geologic setting, mineralogy, metamorphism, geochemistry, and origin: American Mineralogist, v. 90, p. 1473–1499, https://doi.org/10.2138/am.2005.1871.
Klein, C., and Beukes, N.J., 1989, Geochemistry and sedimentology of a facies transition from limestone to iron-formation deposition in the early Proterozoic Transvaal Supergroup, South Africa: Economic Geology, v. 84, p. 1733–1774, https://doi.org/10.2113/gsecongeo.84.7.1733.
Klein, C., and Beukes, N.J., 1993, Sedimentology and geochemistry of the glaciogenic late Proterozoic Rapitan iron-formation in Canada: Economic Geology, v. 88, p. 542–565, https://doi.org/10.2113/gsecongeo.88.3.542.
Knoll, A.H., 1984, The Archean/Proterozoic transition: A sedimentary and paleobiologies perspective, *in* Holland, H.D., and Trendall, A.F., *eds.*, Patterns of Change in Earth Evolution: Dahlem Workshop Reports Physical, Chemical, and Earth Sciences Research Reports, v. 5, Springer, Berlin, p. 221–242, https://doi.org/10.1007/978-3-642-69317-5_13.
Köhler, I., Konhauser, K.O., Papineau, D., Bekker, A., and Kappler, A., 2013, Biological carbon precursor to diagenetic siderite with spherical structures in iron formations: Nature Communications, v. 4, 1741, https://doi.org/10.1038/ncomms2770.
Konhauser, K.O., 2007, Introduction to Geomicrobiology: Blackwell, Oxford. 425 p.
Konhauser, K.O., Hamade, T., Raiswell, R., Morris, R.C., Ferris, F.G., Southam, G., and Canfield, D.E., 2002, Could bacteria have formed the Precambrian banded iron formations?: Geology, v. 30, p. 1079–1082, https://doi.org/10.1130/0091-7613(2002)030<1079:CBHFTP>2.0.CO;2.
Konhauser, K.O., Newman, D.K., and Kappler, A., 2005, The potential significance of microbial Fe(III) reduction during Precambrian banded iron formations: Geobiology, v. 3, p. 167–177, https://doi.org/10.1111/j.1472-4669.2005.00055.x.
Konhauser, K.O., Lalonde, S.V., Amskold, L., and Holland, H.D., 2007a, Was there really an Archean phosphate crisis?: Science, v. 315, 1234, https://doi.org/10.1126/science.1136328.
Konhauser, K.O., Amskold, L., Lalonde, S.V., Posth, N.R., Kappler, A., and Anbar, A., 2007b, Decoupling photochemical Fe(II) oxidation from shallow-water BIF deposition: Earth and Planetary Science Letters, v. 258, p. 87–100, https://doi.org/10.1016/j.epsl.2007.03.026.
Konhauser, K.O., Pecoits, E., Lalonde, S.V., Papineau, D., Nisbet, E.G., Barley, M.E., Arndt, N.T., Zahnle, K., and Kamber, B.S., 2009, Oceanic nickel depletion and a methanogen famine before the Great Oxidation Event: Nature, v. 458, p. 750–753, https://doi.org/10.1038/nature07858.
Konhauser, K.O., Lalonde, S.V., Planavsky, N.J., Pecoits, E., Lyons, T.W., Mojzsis, S.J., Rouxel, O.J., Barley, M.E., Rosière, C., Fralick, P.W., Kump, L.R., and Bekker, A., 2011, Aerobic bacterial pyrite oxidation and acid rock drainage during the Great Oxidation Event: Nature, v. 478, p. 369–373, https://doi.org/10.1038/nature10511.
Konhauser, K.O., Robbins, L.J., Pecoits, E., Peacock, C., Kappler, A., and Lalonde, S.V., 2015, The Archean nickel famine revisited: Astrobiology, v. 15, p. 804–815, https://doi.org/10.1089/ast.2015.1301.
Konhauser, K.O., Planavsky, N.J., Hardisty, D.S., Robbins, L.J., Warchola, T.J., Haugaard, R., Lalonde, S.V., Partin, C.A., Oonk, P.B.H., Tsikos, H., Lyons, T.W., Bekker, A., and Johnson, C.M., 2017, Iron formations: A global record of Neoarchaean to Palaeoproterozoic environmental history: Earth-Science Reviews, v. 172, p. 140–177, https://doi.org/10.1016/j.earscirev.2017.06.012.
Konhauser, K.O., Robbins, L.J., Alessi, D.S., Flynn, S.L., Gingras, M.K., Martinez, R.E., Kappler, A., Swanner, E.D., Li, Y-L., Crowe, S.A., Planavsky, N.J., Reinhard, C.T., and Lalonde, S.V., 2018, Phytoplankton contributions to the trace-element composition of Precambrian banded iron formations: Geological Society of America Bulletin, v. 130, p. 941–951, https://doi.org/10.1130/B31648.1.
Koschwanez, J.H., Foster, K.R., and Murray, A.W., 2011, Sucrose utilization in budding yeast as a model for the origin of undifferentiated multicellularity: PLoS Biology, v. 9, e1001122, https://doi.org/10.1371/journal.pbio.1001122.
Kump, L.R., and Barley, M.E., 2007, Increased subaerial volcanism and the rise of atmospheric oxygen 2.5 billion years ago: Nature, v. 448, p. 1033–1036, https://doi.org/10.1038/nature06058.
Laakso, T.A., and Schrag, D.P., 2018, Limitations on limitation: Global Biogeochemical Cycles, v. 32, p. 486–496, https://doi.org/10.1002/2017GB005832.
Lalonde, S.V., and Konhauser, K.O., 2015, Benthic perspective on Earth's oldest evidence for oxygenic photosynthesis: Proceedings of the National Academy of Sciences, v. 112, p. 995–1000, https://doi.org/10.1073/pnas.1415718112.
Large, R.R., Halpin, J.A., Danyushevsky, L.V., Maslennikov, V.V., Bull, S.W., Long, J.A., Gregory, D.D., Lounejeva, E., Lyons, T.W., Sack, P.J., McGoldrick, P.J., and Calver, C.R., 2014, Trace element content of sedimentary pyrite as a new proxy for deep-time ocean-atmosphere evolution: Earth and Planetary Science Letters, v. 389, p. 209–220, https://doi.org/10.1016/j.epsl.2013.12.020.
Lechte, M., and Wallace, M., 2016, Sub-ice shelf ironstone deposition during the Neoproterozoic Sturtian glaciation: Geology, v. 44, p. 891–894, https://doi.org/10.1130/G38495.1.
Levitus, S., Conkright, M.E., Reid, J.L., Najjar, R.G., and Mantyla, A., 1993, Distribution of nitrate, phosphate and silicate in the world oceans: Progress in Oceanography, v. 31, p. 245–273, https://doi.org/10.1016/0079-6611(93)90003-V.
Li, Y., Sutherland, B.R., Gingras, M.K., Owttrim, G.W., and Konhauser, K.O., 2021, A novel approach to investigate the deposition of (bio)chemical sediments: The sedimentation velocity of cyanobacteria-ferrihydrite aggregates: Journal of Sedimentary Research, v. 91, p. 390–398, https://doi.org/10.2110/jsr.2020.114.
Li, Y.-L., Konhauser, K.O., Cole, D.R., and Phelps, T.J., 2011, Mineral ecophysiological data provide growing evidence for microbial activity in banded-iron formation: Geology, v. 39, p. 707–710, https://doi.org/10.1130/G32003.1.
Li, Y.-L., Konhauser, K.O., Kappler, A., and Hao, X.-L., 2013, Experimental low-grade alteration of biogenic magnetite indicates microbial involvement in generation of banded iron formations: Earth and Planetary Science Letters, v. 361,

p. 229–237, https://doi.org/10.1016/j.epsl.2012.10.025.
Li, Y.-L., Konhauser, K.O., and Zhai, M., 2017, The formation of primary magnetite in the early Archean oceans: Earth and Planetary Science Letters, v. 466, p. 103–114, https://doi.org/10.1016/j.epsl.2017.03.013.
Li, Z.-Q., Zhang, L.-C., Xue, C.-J., Zheng, M.-T., Zhu, M.-T., Robbins, L.J., Slack, J.F., Planavsky, N.J., and Konhauser, K.O., 2018, Earth's youngest banded iron formation implies ferruginous conditions in the Early Cambrian ocean: Scientific Reports, v. 8, 9970, https://doi.org/10.1038/s41598-018-28187-2.
Liu, H., Konhauser, K.O., Robbins, L.J., and Sun, W.D., 2021, Global continental volcanism controlled the evolution of oceanic nickel concentrations: Earth and Planetary Science Letters, v. 572, 117116, https://doi.org/10.1016/j.epsl.2021.117116.
Lovelock, J.E., 1972, Gaia as seen through the atmosphere: Atmospheric Environment (1967), v. 6, p. 579–580, https://doi.org/10.1016/0004-6981(72)90076-5.
Lyons, T.W., Reinhard, C.T., and Planavsky, N.J., 2014, The rise of oxygen in Earth's early ocean and atmosphere: Nature, v. 506, p. 307–315, https://doi.org/10.1038/nature13068.
Mahmoudi, N., Steen, A.D., Halverson, G.P., and Konhauser, K.O., 2023, Biogeochemistry of Earth before exoenzymes: Nature Geosciences, v. 16, p. 845–850, https://doi.org/10.1038/s41561-023-01266-4.
Maliva, R.G., Knoll, A.H., and Simonson, B.M., 2005, Secular change in the Precambrian silica cycle: Insights from chert petrology: Geological Society of America Bulletin, v. 117, p. 835–845, https://doi.org/10.1130/B25555.1.
Mayika, K.B., Moussavou, M., Prave, A.R., Lepland, A., Mbina, M., and Kirsimäe, K., 2020, The Paleoproterozoic Francevillian succession of Gabon and the Lomagundi-Jatuli event: Geology, v. 48, p. 1099–1104, https://doi.org/10.1130/G47651.1.
McNamara, K.J., and Awramik, S.M., 1992, Stromatolites: a key to understanding the early evolution of life: Science Progress, v. 76, p. 345–364, https://www.jstor.org/stable/43421308.
Mloszewska, A.M., Pecoits, E., Cates, N.L., Mojzsis, S.J., O'Neil, J., Robbins, L.J., and Konhauser, K.O., 2012, The composition of Earth's oldest iron-formations: The Nuvvuagittuq supracrustal belt (Quebec, Canada): Earth and Planetary Science Letters, v. 317–318, p. 331–342, https://doi.org/10.1016/j.epsl.2011.11.020.
Mloszewska, A.M., Cole, D.M., Planavsky, N.J., Kappler, A., Whitford, D.S., Owttrim, G.W., and Konhauser, K.O., 2018, UV radiation limited the expansion of cyanobacteria in early marine photic environments: Nature Communications, v. 9, 3008, https://doi.org/10.1038/s41467-018-05520-x.
Morel, F.M.M., and Price, N.M., 2003, The biogeochemical cycles of trace metals in the oceans: Science, v. 300, p. 944–947, https://doi.org/10.1126/science.1083545.
Morris, R.C., 1993, Genetic modelling for banded iron-formations of the Hamersley Group, Pilbara Craton, Western Australia: Precambrian Research, v. 60, p. 243–286, https://doi.org/10.1016/0301-9268(93)90051-3.
Nealson, K.H., and Myers, C.R., 1990, Iron reduction by bacteria: A potential role in the genesis of banded iron formations: American Journal of Science, v. 290, p. 35–45.
Nims, C., and Johnson, J.E., 2022, Exploring the secondary mineral products generated by microbial iron respiration in Archean ocean simulations: Geobiology, v. 20, p. 743–763, https://doi.org/10.1111/gbi.12523.
Olson, S.L., Kump, L.R., and Kasting, J.F., 2013, Quantifying the areal extent and dissolved oxygen concentrations of Archean oxygen oases: Chemical Geology, v. 362, p. 35–43, https://doi.org/10.1016/j.chemgeo.2013.08.012.
Ossa Ossa, F., Hofmann, A., Vidal, O., Kramers, J.D., Belyanin, G., Cavalazzi, B., 2016, Unusual manganese enrichment in the Mesoarchean Mozaan Group, Pongola Supergroup, South Africa: Precambrian Research, v. 281, p. 414–433, https://doi.org/10.1016/j.precamres.2016.06.009.
Ostrander, C.M., Johnson, A.C., and Anbar, A.D., 2021, Earth's first redox revolution: Annual Review of Earth and Planetary Sciences, v. 49, p. 337–366, https://doi.org/10.1146/annurev-earth-072020-055249.
Oze, C., Bird, D.K., and Fendorf, S., 2007, Genesis of hexavalent chromium from natural sources in soil and groundwater: Proceedings of the National Academy of Sciences, v. 104, p. 6544–6549, https://doi.org/10.1073/pnas.0701085104.
Partin, C.A., Bekker, A., Planavsky, N.J., Scott, C.T., Gill, B.C., Li, C., Podkovyrov, V., Maslov, A., Konhauser, K.O., Lalonde, S.V., Love, G.D., Poulton, S.W., and Lyons, T.W., 2013, Large-scale fluctuations in Precambrian atmospheric and oceanic oxygen levels from the record of U in shales: Earth and Planetary Science Letters, v. 369–370, p. 284–293, https://doi.org/10.1016/j.epsl.2013.03.031.
Pecoits, E., Gingras, M.K., Barley, M.A., Kappler, A., Posth, N.R., and Konhauser, K.O., 2009, Petrography and trace element geochemistry of the Dales Gorge banded iron formation: Paragenetic sequence, source and implications for palaeo-ocean chemistry: Precambrian Research, v. 172, p. 163–187, https://doi.org/10.1016/j.precamres.2009.03.014.
Percak-Dennett, E.M., Beard, B.L., Xu, H., Konishi, H., Johnson, C.M., and Roden, E.E., 2011, Iron isotope fractionation during microbial dissimilatory iron oxide reduction in simulated Archaean seawater: Geobiology, v. 9, p. 205–220, https://doi.org/10.1111/j.1472-4669.2011.00277.x.
Peters, S.E., and Loss, D.P., 2012, Storm and fair-weather wave base: A relevant distinction?: Geology, v. 40, p. 511–514, https://doi.org/10.1130/G32791.1.
Planavsky, N.J., Rouxel, O.J., Bekker, A., Lalonde, S.V., Konhauser, K.O., Reinhard, C.T., and Lyons, T.W., 2010, The evolution of the marine phosphate reservoir: Nature, v. 467, p. 1088–1090, https://doi.org/10.1038/nature09485.
Planavsky, N.J., Rouxel, O.J., Bekker, A., Hofmann, A., Little, C.T.S., and Lyons, T.W., 2012a, Iron isotope composition of some Archean and Proterozoic iron formations: Geochimica et Cosmochimica Acta, v. 80, p. 158–169, https://doi.org/10.1016/j.gca.2011.12.001.
Planavsky, N.J., Bekker, A., Hofmann, A., Owens, J.D., and Lyons, T.W., 2012b, Sulfur record of rising and falling marine oxygen and sulfate levels during the Lomagundi event: Proceedings of the National Academy of Sciences, v. 109, p. 18300–18305, https://doi.org/10.1073/pnas.1120387109.
Planavsky, N.J., Asael, D., Hofmann, A., Reinhard, C.T., Lalonde, S.V., Knudsen, A., Wang, X., Ossa Ossa, F., Pecoits, E., Smith, A.J.B., Beukes, N.J., Bekker, A., Johnson, T.M., Konhauser, K.O., Lyons, T.W., and Rouxel, O.J., 2014, Evidence for oxygenic photosynthesis half a billion years before the Great Oxidation Event: Nature Geoscience, v. 7, p. 283–286, https://doi.org/10.1038/ngeo2122.
Planavsky, N., Crowe, S.A., Fakhraee, M., Beaty, B., Reinhard, C.T., Mills, B.J.W., Holstege, C., and Konhauser, K.O., 2021, Evolution of the structure and impact of Earth's biosphere: Nature Reviews Earth & Environment, v. 2, p. 123–139, https://doi.org/10.1038/s43017-020-00116-w.
Posth, N.R., Hegler, F., Konhauser, K.O., and Kappler, A., 2008, Alternating Si and Fe deposition caused by temperature fluctuations in Precambrian oceans: Nature Geoscience, v. 1, p. 703–708, https://doi.org/10.1038/ngeo306.
Posth, N.R., Huelin, S., Konhauser, K.O., and Kappler, A., 2010, Size, density and composition of cell–mineral aggregates formed during anoxygenic phototrophic Fe(II) oxidation: Impact on modern and ancient environments: Geochimica et Cosmochimica Acta, v. 74, p. 3476–3493, https://doi.org/10.1016/j.gca.2010.02.036.
Posth, N.R., Konhauser, K.O., and Kappler, A., 2013a, Microbiological processes in banded iron formation deposition: Sedimentology, v. 60, p. 1733–1754, https://doi.org/10.1111/sed.12051.
Posth, N.R., Köhler, I., Swanner, E.D., Schröder, C., Wellman, E., Binder, B., Konhauser, K.O., Neumann, U., Berthold, C., Nowak, M., and Kappler, A., 2013b, Simulating Precambrian banded iron formation diagenesis: Chemical Geology, v. 362, p. 66–73, https://doi.org/10.1016/j.chemgeo.2013.05.031.
Poulton, S.W., Fralick, P.W., and Canfield, D.E., 2004, The transition to a sulphidic ocean ~1.84 billion years ago: Nature, v. 431, p. 173–177, https://doi.org/10.1038/nature02912.
Prave, A.R., Kirsimäe, K., Lepland, A., Fallick, A.E., Kreitsmann, T., Deines, Yu.E., Romashkin, A.E., Rychanchik, D.V., Medvedev, P.V., Moussavou, M., Bakakas, K., and Hodgskiss, M.S.W., 2022, The grandest of them all: the Lomagundi-Jatuli Event and Earth's oxygenation: Journal of the Geological Society, v.179, p. 2021–2036, https://doi.org/10.1144/jgs2021-036.
Ragsdale, S.W., and Kumar, M., 1996, Nickel-containing carbon monoxide dehydrogenase/acetyl-CoA synthase: Chemical Reviews, v. 96, p. 2515–2540, https://doi.org/10.1021/cr950058+.
Rai, D., Eary, L.E., and Zachara, J.M., 1989, Environmental chemistry of chromium: Science of the Total Environment, v. 86, p. 15–23, https://doi.org/10.1016/0048-9697(89)90189-7.
Rasmussen, B., and Muhling, J.R., 2018, Making magnetite late again: Evidence for widespread magnetite growth by thermal decomposition of siderite in Hamersley banded iron formations: Precambrian Research, v. 306, p. 64–93, https://doi.org/10.1016/j.precamres.2017.12.017.
Rasmussen, B., and Muhling, J.R., 2020, Hematite replacement and oxidative overprinting recorded in the 1.88 Ga Gunflint iron formation, Ontario, Canada: Geology, v. 48, p. 688–692, https://doi.org/10.1130/G47410.1.
Rasmussen, B., Krapež, B., and Meier, D.B., 2014, Replacement origin for hematite in 2.5 Ga banded iron formation: Evidence of postdepositional oxidation of iron-bearing minerals: Geological Society of America Bulletin, v. 126, p. 438–446, https://doi.org/10.1130/B30944.1.
Rasmussen, B., Muhling, J.R., Suvorova, A., and Krapež, B., 2017, Greenalite precipitation linked to the deposition of banded iron formations downslope from a late Archean carbonate platform: Precambrian Research, v. 290, p. 49–62, https://doi.org/10.1016/j.precamres.2016.12.005.

Rasmussen, B., Muhling, J.R., and Krapež, B., 2021a, Greenalite and its role in the genesis of early Precambrian iron formations – A review: Earth-Science Reviews, v. 217, 103613, https://doi.org/10.1016/j.earscirev.2021.103613.

Rasmussen, B., Muhling, J.R., Suvorova, A., and Fischer, W.W., 2021b, Apatite nanoparticles in 3.46–2.46 Ga iron formations: Evidence for phosphorus-rich hydrothermal plumes on early Earth: Geology, v. 49, p. 647–651, https://doi.org/10.1130/G48374.1.

Reddy, T.R., Zheng, X.-Y., Roden, E.E., Beard, B.L., and Johnson, C.M., 2016, Silicon isotope fractionation during microbial reduction of Fe(III)-Si gels under Archean seawater conditions and implications for iron formation genesis: Geochimica et Cosmochimica Acta, v. 190, p. 85–99, https://doi.org/10.1016/j.gca.2016.06.035.

Reinhard, C.T., Raiswell, R., Scott, C., Anbar, A.D., and Lyons, T.W., 2009, A late Archean sulfidic sea stimulated by early oxidative weathering of the continents: Science, v. 326, p. 713–716, https://doi.org/10.1126/science.1176711.

Reinhard, C.T., Planavsky, N.J., Gill, B.C., Ozaki, K., Robbins, L.J., Lyons, T.W., Fischer, W.W., Wang, C., Cole, D.B., and Konhauser, K.O., 2017, Evolution of the global phosphorus cycle: Nature, v. 541, p. 386–389, https://doi.org/10.1038/nature20772.

Rico, K.I., Schad, M., Picard, A., Kappler, A., Konhauser, K.O., and Mahmoudi, N., 2023, Resolving the fate of trace metals during microbial remineralization of phytoplankton biomass in precursor banded iron formation sediments: Earth and Planetary Science Letters, v. 607, 118068, https://doi.org/10.1016/j.epsl.2023.118068.

Robbins, L.J., Lalonde, S.V., Saito, M.A., Planavsky, N.J., Mloszewska, A.M., Pecoits, E., Scott, C., Dupont, C.L., Kappler, A., and Konhauser, K.O., 2013, Authigenic iron oxide proxies for marine zinc over geological time and implications for eukaryotic metallome evolution: Geobiology, v. 11, p. 295–306, https://doi.org/10.1111/gbi.12036.

Robbins, L.J., Swanner, E.D., Lalonde, S.V., Eickhoff, M., Paranich, M.L., Reinhard, C.T., Peacock, C.L., Kappler, A., and Konhauser, K.O., 2015, Limited Zn and Ni mobility during simulated iron formation diagenesis: Chemical Geology, v. 402, p. 30–39, https://doi.org/10.1016/j.chemgeo.2015.02.037.

Robbins, L.J., Lalonde, S.V., Planavsky, N.J., Partin, C.A., Reinhard, C.T., Kendall, B., Scott, C., Hardisty, D.S., Gill, B.C., Alessi, D.S., Dupont, C.L., Saito, M.A., Crowe, S.A., Poulton, S.W., Bekker, A., Lyons, T.W., and Konhauser, K.O., 2016, Trace elements at the intersection of biological and geochemical evolution: Earth-Science Reviews, v. 163, p. 323–348, https://doi.org/10.1016/j.earscirev.2016.10.013.

Robbins, L.J., Konhauser, K.O., Warchola, T.J., Homann, M., Thoby, M., Foster, I., Mloszewska, A.M., Alessi, D.S., and Lalonde, S.V., 2019a, A comparison of bulk versus laser ablation trace element analyses in banded iron formations: Insights into the mechanisms leading to compositional variability: Chemical Geology, v. 506, p. 197–224, https://doi.org/10.1016/j.chemgeo.2018.12.036.

Robbins, L.J., Funk, S.P., Flynn, S.L., Warchola, T.J., Li, Z., Lalonde, S.V., Rostron, B.J., Smith, A.J.B., Beukes, N.J., de Kock, M.O., Heaman, L.M., Alessi, D.S., and Konhauser, K.O., 2019b, Hydrogeological constraints on the formation of Palaeoproterozoic banded iron formations: Nature Geoscience, v. 12, p. 558–563, https://doi.org/10.1038/s41561-019-0372-0.

Robbins, L.J., Fakhraee, M., Smith, A.J.B., Bishop, B.A., Swanner, E.D., Peacock, C.L., Wang, C.-L., Planavsky, N.J., Reinhard, C.T., Crowe, S.A., and Lyons, T.W., 2023, Manganese oxides, Earth surface oxygenation, and the rise of oxygenic photosynthesis: Earth-Science Reviews, v. 239, 104368, https://doi.org/10.1016/j.earscirev.2023.104368.

Rosing, M.T., and Frei, R., 2004, U-rich Archaean sea-floor sediments from Greenland – indications of >3700 Ma oxygenic photosynthesis: Earth and Planetary Science Letters, v. 217, p. 237–244, https://doi.org/10.1016/S0012-821X(03)00609-5.

Saito, M.A., Sigman, D.M., and Morel, F.M.M., 2003, The bioinorganic chemistry of the ancient ocean: the co-evolution of cyanobacterial metal requirements and biogeochemical cycles at the Archean–Proterozoic boundary?: Inorganica Chimica Acta, v. 356, p. 308–318, https://doi.org/10.1016/S0020-1693(03)00442-0.

Sánchez-Baracaldo, P., 2015, Origin of marine planktonic cyanobacteria: Scientific Reports, v. 5, 17418, https://doi.org/10.1038/srep17418.

Sánchez-Baracaldo, P., Bianchini, G., Wilson, J.D., and Knoll, A.H., 2022, Cyanobacteria and biogeochemical cycles through Earth history: Trends in Microbiology, v. 30, p. 143–157, https://doi.org/10.1016/j.tim.2021.05.008.

Schad, M., Halama, M., Bishop, B., Konhauser, K.O., and Kappler, A., 2019a, Temperature fluctuations in the Archean ocean as trigger for varve-like deposition of iron and silica minerals in banded iron formations: Geochimica et Cosmochimica Acta, v. 265, p. 386–412, https://doi.org/10.1016/j.gca.2019.08.031.

Schad, M., Konhauser, K.O., Sánchez-Baracaldo, P., Kappler, A., and Bryce, C., 2019b, How did the evolution of oxygenic photosynthesis influence the temporal and spatial development of the microbial iron cycle on ancient Earth?: Free Radical Biology and Medicine, v. 140, p. 154–166, https://doi.org/10.1016/j.freeradbiomed.2019.07.014.

Schad, M., Byrne, J.M., ThomasArrigo, L.K., Kretzschmar, R., Konhauser, K.O., and Kappler, A., 2022, Microbial Fe cycling in a simulated Precambrian ocean environment: Implications for secondary mineral (trans)formation and deposition during BIF genesis: Geochimica et Cosmochimica Acta, v. 331, p. 165–191, https://doi.org/10.1016/j.gca.2022.05.016.

Schidlowski, M., Eichmann, R., and Junge, C.E., 1976, Carbon isotope geochemistry of the Precambrian Lomagundi carbonate province, Rhodesia: Geochimica et Cosmochimica Acta, v. 40, p. 449–455, https://doi.org/10.1016/0016-7037(76)90010-7.

Schirrmeister, B.E., de Vos, J.M., Antonelli, A., and Bagheri, H.C., 2013, Evolution of multicellularity coincided with increased diversification of cyanobacteria and the Great Oxidation Event: Proceedings of the National Academy of Sciences, v. 110, p. 1791–1796, https://doi.org/10.1073/pnas.1209927110.

Scott, C., Wing, B.A., Bekker, A., Planavsky, N.J., Medvedev, P., Bates, S.M., Yun, M., and Lyons, T.W., 2014, Pyrite multiple-sulfur isotope evidence for rapid expansion and contraction of the early Paleoproterozoic seawater sulfate reservoir: Earth and Planetary Science Letters, v. 389, p. 95–104, https://doi.org/10.1016/j.epsl.2013.12.010.

Siever, R., 1992, The silica cycle in the Precambrian: Geochimica et Cosmochimica Acta, v. 56, p. 3265–3272, https://doi.org/10.1016/0016-7037(92)90303-Z.

Simonson, B.M., and Goode, A.D.T., 1989, First discovery of ferruginous chert arenites in the early Precambrian Hamersley Group of Western Australia: Geology, v. 17, p. 269–272, https://doi.org/10.1130/0091-7613(1989)017%3C0269:FDOFCA%3E2.3.CO;2.

Simonson, B.M., and Hassler, S.W., 1996, Was the deposition of large Precambrian iron formations linked to major marine transgressions?: The Journal of Geology, v. 104, p. 665–676, https://www.jstor.org/stable/30081160.

Smedley, P.L., and Kinniburgh, D.G., 2002, A review of the source, behaviour and distribution of arsenic in natural waters: Applied Geochemistry, v. 17, p. 517–568, https://doi.org/10.1016/S0883-2927(02)00018-5.

Smith, A.J.B., 2018, The iron formations of southern Africa, *in* Siegesmund, S., Basei, M.A.S., Oyhantçabal, P., and Oriolo, S., *eds.*, Geology of Southwest Gondwana: Regional Geology Reviews, Springer, Cham, p. 469–491, https://doi.org/10.1007/978-3-319-68920-3_17.

Smith, A.J.B., and Beukes, N.J., 2023, The paleoenvironmental implications of pre-Great Oxidation Event manganese deposition in the Mesoarchean Ijzermijn Iron Formation Bed, Mozaan Group, Pongola Supergroup, South Africa: Precambrian Research, v. 384, 106922, https://doi.org/10.1016/j.precamres.2022.106922.

Smith, A.J.B., Beukes, N.J., and Gutzmer, J., 2013, The composition and depositional environments of Mesoarchean iron formations of the West Rand Group of the Witwatersrand Supergroup, South Africa: Economic Geology, v. 108, p. 111–134, https://doi.org/10.2113/econgeo.108.1.111.

Smith, A.J.B., Beukes, N.J., Gutzmer, J., Czaja, A.D., Johnson, C.M., and Nhleko, N., 2017, Oncoidal granular iron formation in the Mesoarchaean Pongola Supergroup, southern Africa: Textural and geochemical evidence for biological activity during iron deposition: Geobiology, v. 15, p. 731–749, https://doi.org/10.1111/gbi.12248.

Smith, A.J.B., Beukes, N.J., Cochrane, J.M., Gutzmer, J., 2023, Manganese carbonate-bearing mudstone of the Witwatersrand-Mozaan succession in southern Africa as evidence for bacterial manganese respiration and availability of free molecular oxygen in Mesoarchaean oceans: South African Journal of Geology, v. 126, p. 29–48, https://doi.org/10.25131/sajg.126.0005.

Søgaard, E.G., Medenwaldt, R., and Abraham-Peskir, J.V., 2000, Conditions and rates of biotic and abiotic iron precipitation in selected Danish freshwater plants and microscopic analysis of precipitate morphology: Water Research, v. 34, p. 2675–2682, https://doi.org/10.1016/S0043-1354(00)00002-6.

Steinhoefel, G., von Blackenburg, F., Horn, I., Konhauser, K.O., Beukes, N.J., and Gutzmer, J., 2010, Deciphering formation processes of banded iron formations from the Transvaal and the Hamersley successions by combined Si and Fe isotope analysis using UV femtosecond laser ablation: Geochimica et Cosmochimica Acta, v. 74, p. 2677–2696, https://doi.org/10.1016/j.gca.2010.01.028.

Sumner, D.Y., 1997, Carbonate precipitation and oxygen stratification in late Archean seawater as deduced from facies and stratigraphy of the Gamohaan and Frisco formations, Transvaal Supergroup, South Africa: American Journal of Science, v. 297, p. 455–487, https://doi.org/10.2475/ajs.297.5.455.

Sumner, D.Y., and Beukes, N.J., 2006, Sequence stratigraphic development of the Neoarchean Transvaal carbonate platform, Kaapvaal, Craton, South Africa:

South African Journal of Geology, v. 109, p. 11–22, https://doi.org/10.2113/gssajg.109.1-2.11.

Sun, S., Konhauser, K.O., Kappler, A., and Li, Y.-L., 2015, Primary hematite in Neoarchean to Paleoproterozoic oceans: Geological Society of America Bulletin, v. 127, p. 850–861, https://doi.org/10.1130/B31122.1.

Sunda, W.G., 2012, Feedback interactions between trace metal nutrients and phytoplankton in the ocean: Frontiers in Microbiology, v. 3, 204, https://doi.org/10.3389/fmicb.2012.00204.

Swanner, E.D., Mloszewska, A.M., Cirpka, O.A., Schoenberg, R., Konhauser, K.O., and Kappler, A., 2015, Modulation of oxygen production in Archaean oceans by episodes of Fe(II) toxicity: Nature Geoscience, v. 8, p. 126–130, https://doi.org/10.1038/ngeo2327.

Thompson, K.J., Kenward, P.A., Bauer, K.W., Warchola, T., Gauger, T., Martinez, R., Simister, R.L., Michiels, C.C., Llirós, M., Reinhard, C.T., Kappler, A., Konhauser, K.O., and Crowe, S.A., 2019, Photoferrotrophy, deposition of banded iron formations, and methane production in the Archean oceans: Science Advances, v. 5, eaav2869, https://doi.org/10.1126/sciadv.aav2869.

Tosca, N.J., and Tutolo, B.M., 2023, Hydrothermal vent fluid-seawater mixing and the origins of Archean iron formation: Geochimica et Cosmochimica Acta, v. 352, p. 51–68, https://doi.org/10.1016/j.gca.2023.05.002.

Tréguer, P., Nelson, D.M., Van Bennekom, A.J., DeMaster, D.J., Leynaert, A., and Quéguiner, B., 1995, The silica balance in the world ocean: A reestimate: Science, v. 268, p. 375–379, https://doi.org/10.1126/science.268.5209.375.

Trendall, A.F., 2002, The significance of iron-formation in the Precambrian stratigraphic record, *in* Altermann, W., and Corcoran, P.L., *eds.,* Precambrian Sedimentary Environments: A Modern Approach to Ancient Depositional Systems: International Association of Sedimentologists Special Publications, v. 33, p. 33–66, https://doi.org/10.1002/9781444304312.ch3.

Trendall, A., and Blockley, J., 1970, The Iron Formations of the Precambrian Hamersley Group, Western Australia with Special Reference to the Associated Crocidolite: Western Australia Geological Survey Bulletin, v. 119, 366 p.

Tyrrell, T., 1999, The relative influences of nitrogen and phosphorus on oceanic primary production: Nature, v. 400, p. 525–531, https://doi.org/10.1038/22941.

Tyson, R.V., and Pearson, T.H., 1991, Modern and ancient continental shelf anoxia: an overview: Geological Society, London, Special Publications, v. 58, p. 1–24, https://doi.org/10.1144/GSL.SP.1991.058.01.01.

Walker, J.C.G., 1984, Suboxic diagenesis in banded iron formations: Nature, v. 309, p. 340–342, https://doi.org/10.1038/309340a0.

Weber, M.F., Poxleitner, G., Hebisch, E., Frey, E., and Opitz, M., 2014, Chemical warfare and survival strategies in bacterial range expansions: Journal of the Royal Society Interface, v. 11, 20140172, https://doi.org/10.1098/rsif.2014.0172.

Whitehouse, M.J., and Fedo, C.M., 2007, Microscale heterogeneity of Fe isotopes in >3.71 Ga banded iron formation from the Isua Greenstone Belt, southwest Greenland: Geology, v. 35, p. 719–722, https://doi.org/10.1130/G23582A.1.

Widdel, F., Schnell, S., Heising, S., Ehrenreich, A., Assmus, B., and Schink, B., 1993, Ferrous iron oxidation by anoxygenic phototrophic bacteria: Nature, v. 362, p. 834–836, https://doi.org/10.1038/362834a0.

Wu, X., Zhu, J., He, H., Xian, H., Yang, Y., Ma, L., Liang, X., Lin, X., Li, S., Konhauser, K.O., and Li, Y., 2023, Geodynamic oxidation of the Archean terrestrial surfaces: Communications Earth & Environment, v. 4,132, https://doi.org/10.1038/s43247-023-00789-3.

Zahnle, K.J., Claire, M., and Catling, D., 2006, The loss of mass-independent fractionation in sulfur due to a Palaeoproterozoic collapse of atmospheric methane: Geobiology, v. 4, p. 271–283, https://doi.org/10.1111/j.1472-4669.2006.00085.x.

Zerkle, A.L., House, C.H., and Brantley, S.L., 2005, Biogeochemical signatures through time as inferred from whole microbial genomes: American Journal of Science, v. 305, p. 467–502, https://doi.org/10.2475/ajs.305.6-8.467.

Zheng, X.-Y., Beard, B.L., Reddy, T.R., Roden, E.E., and Johnson, C.M., 2016, Abiologic silicon isotope fractionation between aqueous Si and Fe(III)-Si gel in simulated Archean seawater: Implications for Si isotope records in Precambrian sedimentary rocks: Geochimica et Cosmochimica Acta, v. 187, p. 102–122, https://doi.org/10.1016/j.gca.2016.05.012.

Received August 2023
Accepted as revised October 2023